Photocopy and Use Authorization

In presenting this thesis in partial fulfillment of the requirements for an advanced degree at Idaho State University, I agree that the library shall make free inspection. I further state the permission for extensive copying of this dissertation for scholarly purposes may be granted by the Dean of the Graduate Studies, Dean of the College of Engineering, or by the University Librarian. It is understood that any copying and publication of this dissertation for financial gain shall not be allowed without my written permission.

Signature____

Date____

Stall Predication in Jet Compressor Blades Using Autocorrelation and ESD Model

by

Ali Albeesh

A thesis

submitted in partial fulfillment

of the requirements for the degree of

Master of Science in the Department of Mechanical Engineering

Idaho State University

Fall 2020

To the Graduate Faculty:

The committee members appointed to examine the thesis of Ali Albeesh find it satisfactory and recommend that it be accepted.

____

Dr. Marco P. Schoen, Major Advisor

____

Dr. Bosworth Kenneth W Co-Advisor

____

Dr. Mahar, James W, GFR

Acknowledgement

I want to extend special thanks to my principal advisor Dr. Marco P. Schoen, to give this opportunity to work in this significant research and for hid assistance and guidance in completing this thesis. I could not accomplish this success in my career without his motivation and support this research would not have been possible existed.

I would also like to give special thanks to my professor Marry Hofle for her support. Special thanks for my friend Berith A.Sanchez for all his help and motivation, and my wonderful girlfriend Bryanna Adermenn for unlimited patience. Without them this research would not have been possible. I want to give a huge thanks to the Jet Engine Club at Idaho State University and special thanks to the people who help make this jet engine running and make the dream of collecting data at the university comes true. I want to give special thanks to the jet engine club's members, especially the jet engine senior design project Zak Macpherson and Carl Crome. Moreover, a special thanks to Mike Crump that this project would not exist without his welding skills and hard work.

Table of Contents

List of Figures

List of Tables

Stall Predication in Jet Compressor Blades Using Autocorrelation and ESD Model

Thesis Abstract—Idaho State University (2020)

It is complicated to run a jet engine at a high efficiency during the start-up as the RPM of the system increases without exhibiting stall in the jet's compressor section. When the compressor system approaches the maximum efficiency, the pressure rise is at its optimum, however stall may occur. Most of the research published on this topic provides essential information on the spike stall. Some research reported precursors to indicate stall 100 to 220 revolutions before the event of stall. However, this is associated with modal stall inception. Stall happens in the first stage of the system and if not mitigated can cause severe damage to the system. In this thesis, a numerical method for stall precursor detection is investigated utilizing real compressor test data. . In this thesis, three different methods are utilized for the purpose to find precursors of stall: the Generalized Extreme Studentized Deviate Test (ESD) and Autoregressive models (AR).

Key Words: Jet engine, Stall prediction, Generalized Extreme Studentized Deviate Test, Autoregressive models.

1.0 Chapter One

1.1 Introduction

The compressor of a jet engine is impossibly to run with high efficiency because of safety concerns. Safety is primarily defined by the engine not going into stall or into surge. The surge and stall both lead to unstable flow compressor see Figure 1. As it is shown in the figure the

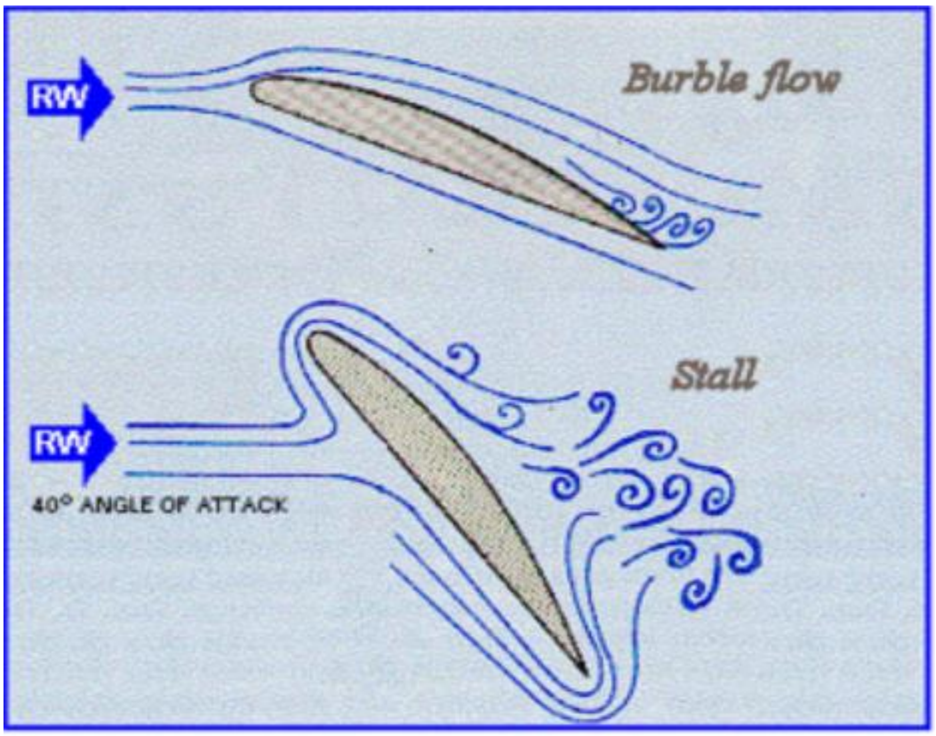

Figure 1 Spike-Stall Formation [1].

disturbance of the flow inside the compressor is an angle direction which is the stall. However, the surge is the disturbance of compressor flow in the axial direction. The stall in the axial compressor transfers the inlet flow from a regular burble flow to stall flow as show in figure 1. The stall essentially blocks the flow within a blade section. As the incoming fluid starts bypassing that passage, it increases the air flow in the adjacent passages, and hence causing stall at those instances. As this process repeats itself, it generates a stall that travels in a circumferential manner around the compressor stage, hence the name rotating stall. Many research studies have been developed to study spike stall and surge phenomena since the early development of the gas jet engine operation. The spike stall is one of the reasons why the compressor of a jet engine may not run at a high efficiency. Improving the compressor's efficiency in the jet engine has been a research target since the first jet engines have been developed. Increasing the jet engine's operating efficiency implies that the stall problem inside the compressor needs to be observed and solved. The stall phenomenon in the different stages of the compressor system has been linked to the jet engine's efficiency. There are many different causes of spike stall formation Many researchers use control system methods to inspect and mitigate the stall formation problem. Additionally, such methods and algorithms allow for the investigation on why stall occurs in axial compressors. The researchers study the change in pressure and velocity to characterize the behavior in the compressor system's different stages in order to understand the stall problem. Much research developed different methods to understand the spike stall phenomenon, however, there still exists much unknowns and a number of phenomena are still not well understood [2].

The changes in the fluid dynamics within the engine influences the operation of the jet engine and is one of the main reasons for stall formation. The impact of the changed fluid dynamics of the air flow within the compressor causes a change of the flow within the blade passage and increases the likelihood of stall formation. The change in the air flow within the blade passage of the compressor rotor changes the air mass that causes an impact on the engine operation stability and performance. The change in the engine operation and its behavior can be studied using software and mathematical models, which is a part of this thesis work. Such endeavors use an expansive experimental test base in order to understand stall issues. The experimental data is used to develop numerical simulations to study and predict flow in the blade passage and predict stall. The rotating spike stall is one of the main reasons the jet engine runs at moderate efficiency. Different methods were developed to understand the spike stall formation. However, one of the more promising approaches to investigate the stall formation is simulation based on acquired data. It is crucial to understand the spike stall formation issues to improve the jet engine compressor's efficiency. For example, according to S.R. Montgomery, the rotating stall is a region of separated flow, moving relative to a blade row [3]. Montgomery used computer software to implement mathematical models in order to realize numerical experiments for the purpose to predict the spike stall frequency. Hence, it is possible to design anti-spike stall blades [3].

2.0 Chapter Two

2.1 Operation of jet engine/compressor

A jet engine consists of five mains components. It is built up by a compressor, a combustion chamber, a turbine section, and the exhaust nozzle as shown in Figure 2. The operation of the gas jet engine is based on

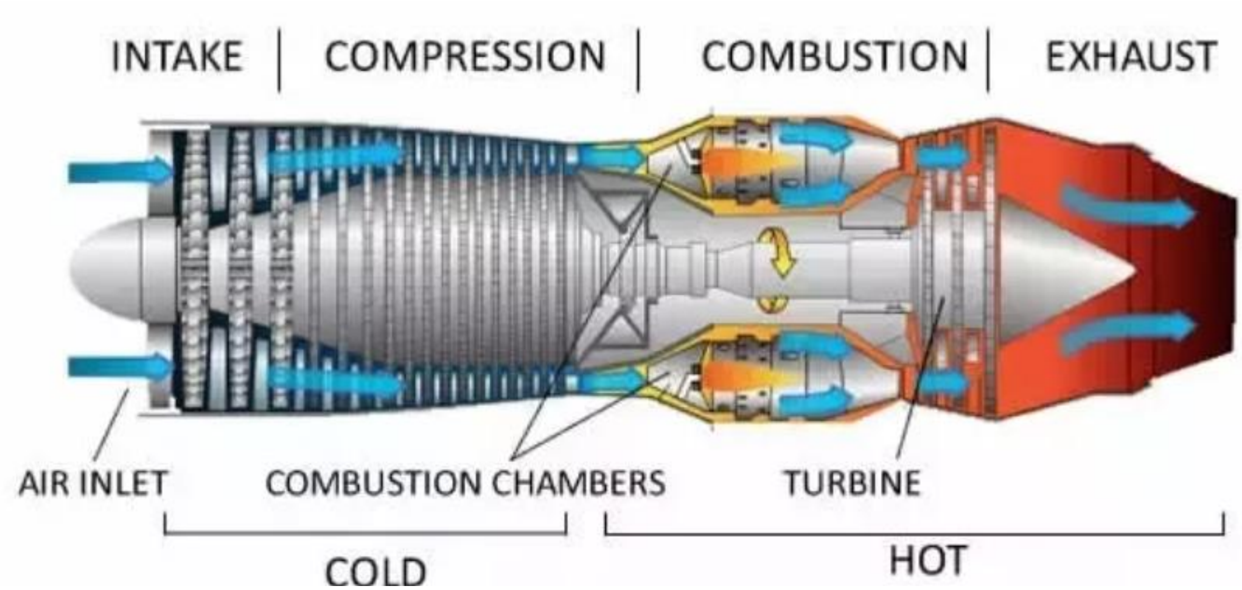

Figure 2. Jet engine J34 WE-36 [22]

Newton Third Law, which is "if a body exerts a force on a second body, the second body exerts a force that is equal in magnitude and opposite in direction to the first force" [5]. Therefore, for every action there is a reaction force that is equal to the action [5]. The relationship between the velocity and the inputs is direct relationship. For the gas jet engine to run, it needs cold air to be compressed to very high pressure and heated to very high temperature to create a very powerful push force that is capable to move a big airplane with very large speed. For this operation, each component of the jet engine has a role for this operation to be running.

2.1.1 Jet engine component parts roles

The first part of the jet engine is the inlet vane assembly as shown in Figure 3, the inlet vane is a single compressor stage and is comprised of a spinning rotor paired with a ring of stationary stator vanes. The stationary stators vans and stationary stators compressor are attached to the core casing. The inlet vanes rotor blades swirl the air as they force it through the compressor.

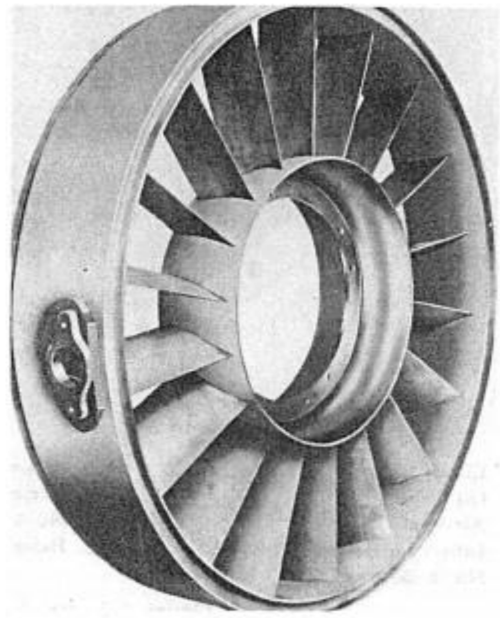

Figure 3 Inlet Vane assembly [4].

The compressor is consisting of different number of stages and each stage of the compressor has a stage stator and a rotor. Each stage is compressing the air by a specific ratio, mostly by a 1 to 1.25 ratio Figure 4. Over a number of stages, the compressor is capable of producing very high-pressures of

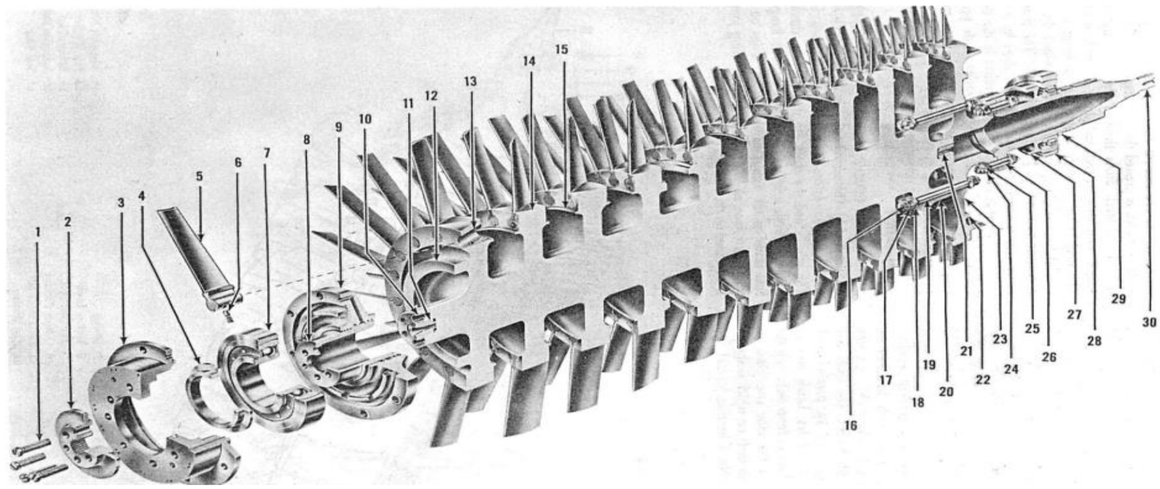

Figure 4 Aluminum Compressor Rotor Cutaway [4].

air and force it to the outlet guide ring to direct the compression air to the diffuser. Now the air is in the midframe of the jet engine's the diffuser as shown in Figure 5 which contains the liquid fuel nozzle to inject fuel directly to the combustor can. The combustor is where cold air is mixed with fuel and ignited as the air passes through the combustor, releasing a jet of high-power gas. The combustor contains cooling holes as shown in Figure 5 for cooling air to mix with flames. The air

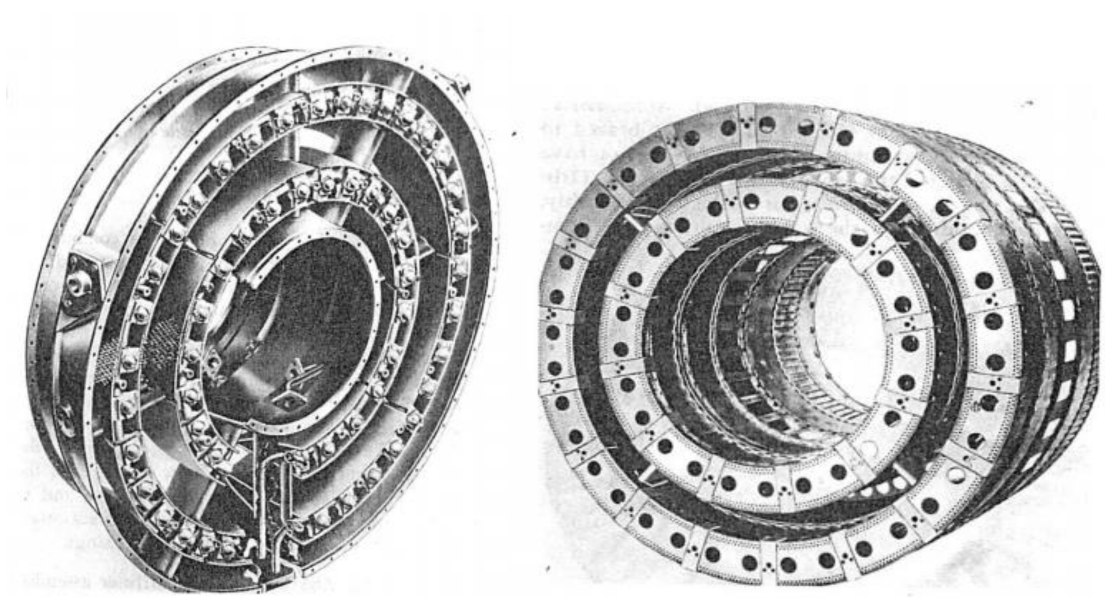

Figure 5 Diffuser Cutaway and Combustion Chamber Line [4].

leaves the combustor through a transaction ring that turns the cylindrical combustor outlet to a ring of hot gases. The holes in the surface of the diffuser are called the cooling holes, as shown in Figure 5. The role of the cooling hole is to keep the surface in the regular temperature operation. The hot gases are forced to specific directions to hit the turbine blade using the nozzle and that causes the turbine to start turning. The turbine contains a second stage nozzle to lead the gases to the second stage of the turbine as shown in Figure 6.. The exhaust nozzle or the afterburner is

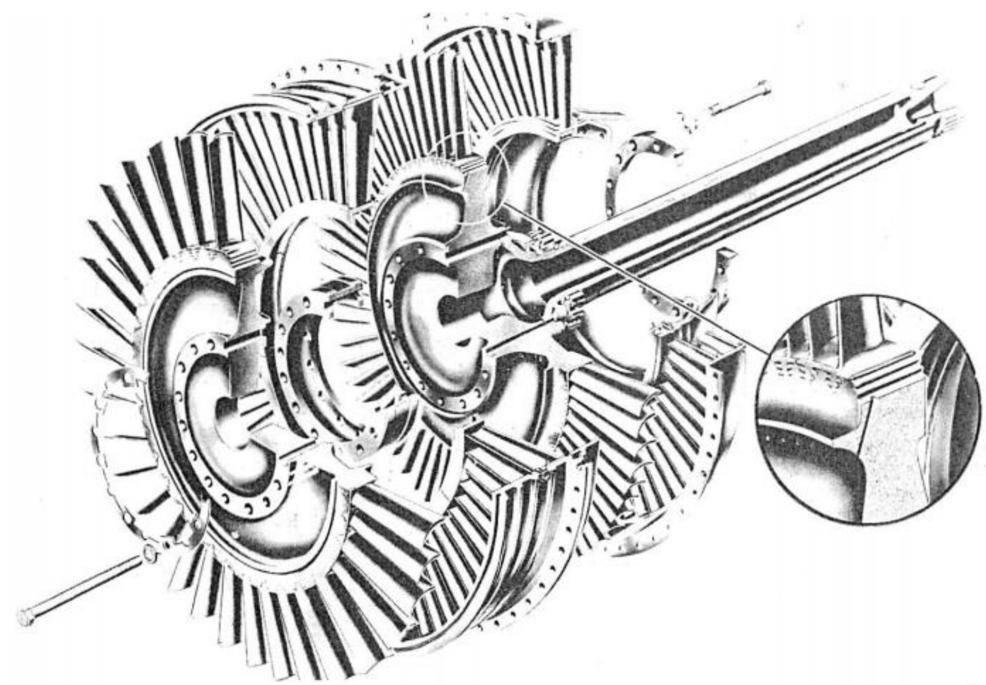

Figure 6 Turbine Section Cutaway [4].

located behind the core of the jet engine right in front the jet shaft, the exhaust nozzle is to create high velocity when the compressed gas mixture pass through Figure 7.

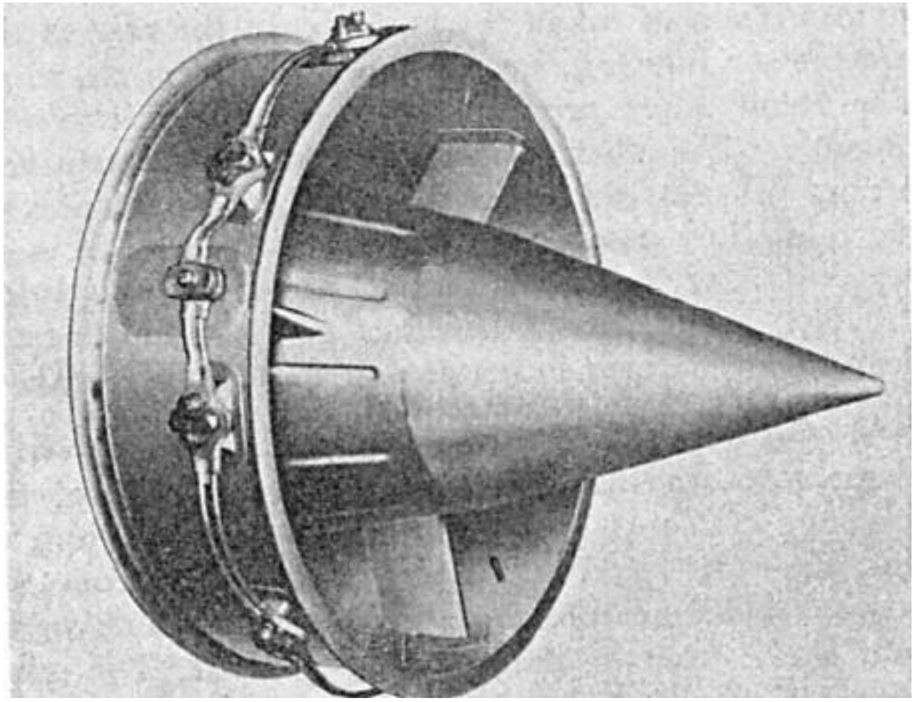

Figure 7 Exhaust Collector with Attached Thermocouples [4].

2.2 Problem Statement

2.2.1 Stall explanations and how it effects on engine performance

Since the development of the gas jet engine, the spike stall problem limits the efficiency of the turbomachinery process at approximately 64% efficiency. As the air pressure compression increase and the engine of the jet engine start suffering from stall as the airflow change angle direction [6]. The performance of the jet engine has an opposite relationship with pressure rise and spike stall formation as shown in Figure 8 [6]. It is complicated to study the causes of the

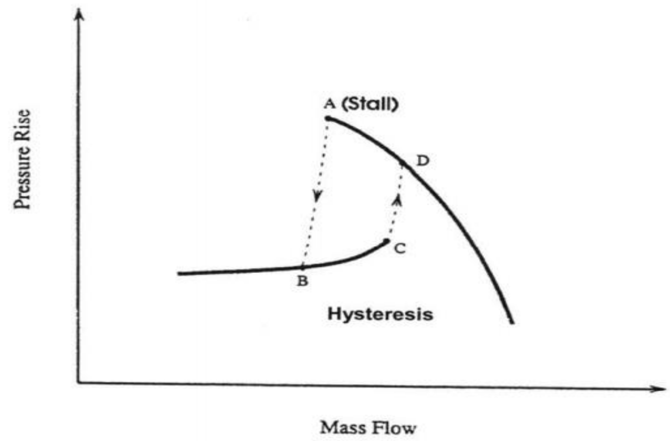

Figure 8 Effect of rotating stall in compressor efficiency [6].

spike stall problem, and it is still not fully understood, although researchers have been studying this problem since the invention of the gas jet engine. According to Huu "the rotating stall is a compressor instability characterized by the formation of a cell of velocity deficiency that rotates at speed from 15-50% of the compressor rotor speeds as shown in Figure 9 below "[6]. Studying

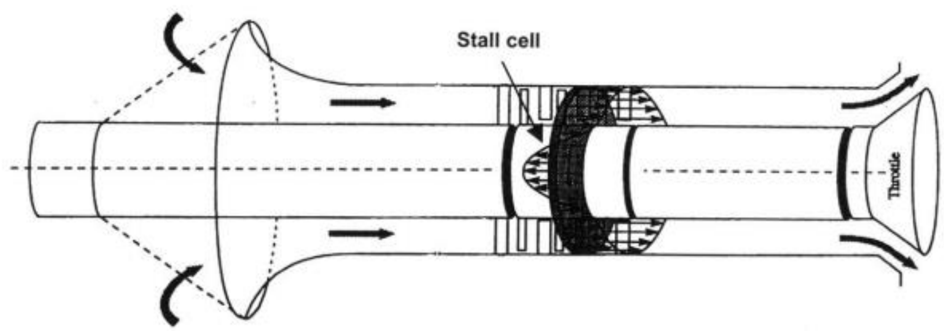

Figure 9 Stall cell formation [6].

jet engine flow dynamics is very complicated, particularly the understanding of the causes of spike stall. Since 1960, many researchers have tried to diagnose the causes of spike stall on the leading edge of the rotor blades of the first stage of an axial compressor, but it is not fully understood yet. Spike stall happens at the edge of the compressor's blade and increases because of the complete disruption of the airflow in the blade passage. The spike stall problem occurs when the gas jet engine runs at high efficiency, so it limits the compressor to run at optimum efficiency. The jet engine cannot work at high efficiency without increasing the possibility of spike stall formation. The flow dynamics inside the compressor and the high pressure resulting in the spike stall formation develops because the compressor approaches instability at the peak of the efficiency curve, as shown in Figure 8. To understand the relationship between the increase of the gas jet engine's running efficiency and the spike stall formation, it is essential to study the compressor's flow dynamics. For this purpose, it is possible to collect pressure and velocity data points experimentally and develop numerical simulation to determine the causes of spike stall formation inside the blade passage.

2.2.2 Spike stall type

There are different aspects involved in collecting and observing pressure data. An important aspect is the position of the sensor with respect to the stator blades, according to [7]. Compressor stability blades have curved profiles of four-digit series with ten percent thickness. The first digit is to define the maximum camber as percentage of the chord. The second digit is to indicate the distance of maximum camber form the airfoil leading edge in tenths of the chord as shown in figure 10. The last two digits is describing the maximum thickness of the airfoil as precent of the chord as shown in Figure 10. The rules are to mount the sensors in the vicinity of a stall region in

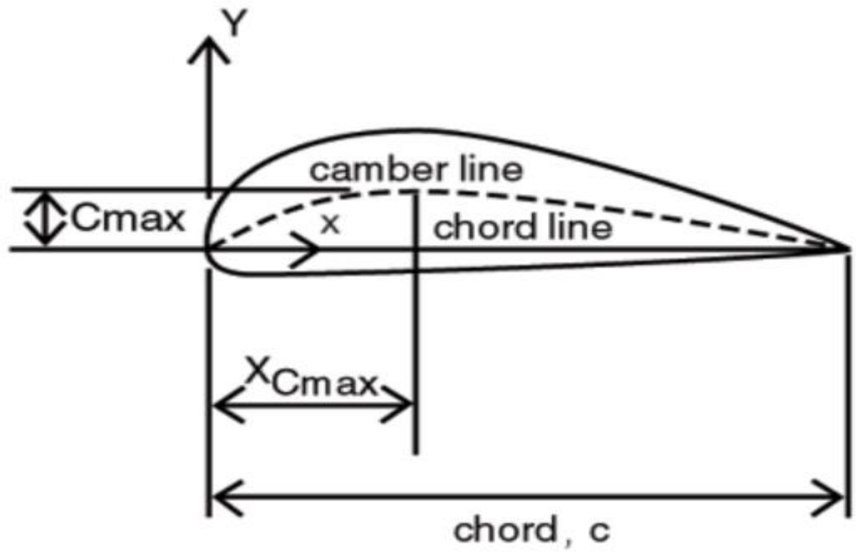

Figure 10 Four-digit system describe an airfoil section [8].

order to measure the velocity or pressure. When the measurement is collected, it is possible to develop a simulation application to predict spike stall in the compressor between the impeller and vanned diffuser area in a gas jet engine. The measurement is collected to help identify the spike stall type. There are two stall types, the long length-scale or modal inception and short length-scale od spike inception [6].The spike stall forms at the limits the compressor performance, running at high efficiency. Since the invention of the jet engine, there has been much research to try to understand the spike stall problem in order to increase the efficacy of the operation of the jet engine. However, this problem is still not well understood. Many researchers have developed a simulation application to investigate the causes of the spike stall formation, including the discovery of the change in the flow dynamic properties of the fluids inside the compressor, for instance Stephen R. Montgomery in 1955. Indeed, the change of the fluid's properties, such as the pressure, temperature, or velocity, is the leading candidate to detect the formation of spike stall in the compressor's first stage [9]. Researchers have found that the spike stall always starts to form in the first stage of the compressor.

2.2.3 Causes of spike stall

The air flow enters the compressor at a constant speed while the mass flow of the air is reduced and the pressure rise significantly in short period of time to the point where instabilities occurs as shown in Figure 11 [6]. The instabilities occur in the flow inside the compressor is the rotating

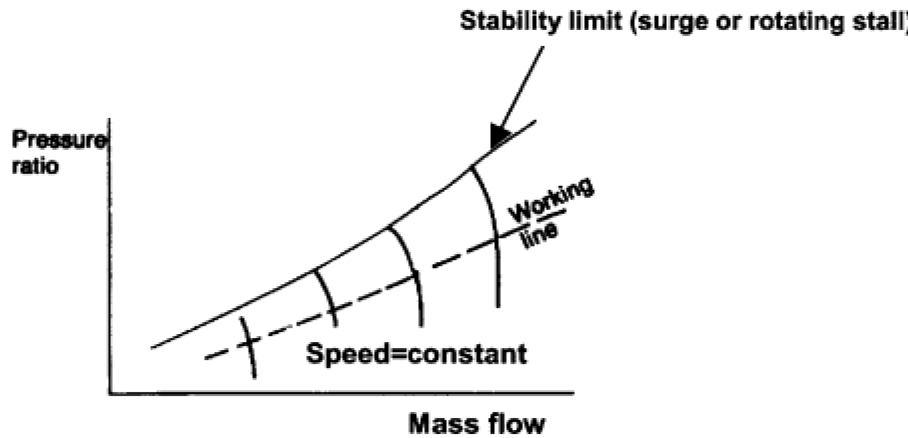

Figure 11 Compressor stability limits [6].

stall or surge, except surge on one-dimensional axisymmetric flow. The spike stall problem is happening in axial compressors and the main reason of spike stall formation is the region of separated flow. As show in figure 11, the stability region of the pressure compression ratio inside the compressor crosses the stability limit and surge or rotating stall occurs. Many studies indicate the relationship between the rotating stall at the blade's tip and the aerodynamic flow within the compressor [10]. The spike stall formation is a vibration problem since the resulting vibration causes severe blade stress to be imposed at low mass flow conditions [11]. The resulting vibration cause aerodynamic instabilities in the axial compressor of the jet engine. The instability of the aerodynamic flow can happen in different stages of the compressor system, but most of the time starts in the first stage. In 2004 research was proposed to identify spike stall in compressor systems using autocorrelation by attaching pressure sensors in the casing close to the tip of the leading edge of the first row of the compressor [12]. The influence of unsteady flow structures in the tip region is responsible for the extension of the compressor stall margin [12]. Another study showed that the compression of the gas inside of the axial compressor of a jet engine suffers from the aerodynamic instabilities [11]. The aerodynamic of the fluid in the compression section at low mass flow rates exhibits stall pre-cursors within the blade passage fluid flow.

Previous research has resulted in a numerical method to study the aerodynamics in an axial compressor to investigate the spike stall frequency [13]. If the spike stall at a given rotor frequency can be predicted, then control interactions such as air injection can reduce the effects or eliminate the inception of stall. For example, Pullan et al. investigated the spike stall critical frequency in axial compressors [13]. This investigation utilized experimental measurements and numerical simulation. In 2015, Pullan et al. studied spike stall by combining both measurements and simulation work together [13]. The formation of a spike stall has also been investigated experimentally in single stage machine by Massachusetts Institute of Technology. They studied the spike stall formation problem numerically in different machines by studying the flow field and measure the pressure fluctuation. These formations of flow structures are the main reason for the formation of spike stall within the blade passages [10]. In their work, the numerical calculation experiment is developed to predict the rotating stall which can help in predicting the spike stall formation.

2.3 Objective

In this work, pressure data was utilized to test a new stall prediction algorithm on a one stage and a three-stages compressor system. The algorithm utilizes an Auto Regressive (AR) model to capture the pressure data. This dynamic model is further analyzed by observing the eigenvalues of the AR model over time and track the changes in magnitude of these eigenvalues. A statistical outlier algorithm is employed to determine when an eigenvalue becomes dominant in terms of change, indicating stall may occur if the compressor is operated at this configuration.

The objectives of this thesis are to modify a Westinghouse J-34 jet engine in order to be able to install a sensor system for studying different stall formation conditions and for developing simulations to predict spike stall. The developed numerical outlier detection algorithm involving the AR model and the ESD test is a candidate for being applied to the test system once completed. As this project is a multi-member project, portions of the tasks were part of this thesis work. Ongoing work in implementing the sensor system will ultimately yield an opportunity to test and develop such stall precursors algorithms and compare existing algorithms. For safety reasons, the jet engine was modified to run using an electric motor with VFD drive. The system was designed by a senior design group and was modified to accommodate the testing plan of the proposed algorithm detailed in this thesis.

3.0 Chapter Three

3.1 Proposed algorithms to detect stall

Research studies have reported several approaches to avoid the flow instability inside the compression system of the gas jet engines. Stanning's theory, for example, used pressure data to compute the autocorrelation of the measured pressure of the same blade passage after each revolution. The study implemented active flow control, where air was injected to the tip of the blade passage. In 1993 Paduano at al. tested a technique of a one-dimension nonlinear approach implemented to indicate stall with flow recirculation and injection to increase the peak pressure by 25%. [3]. The pressure fluctuation caused by rotating stall was less downstream of the rotor than upstream. The pressure fluctuation develops by the aerodynamic instabilities in axial compressors, and it is essential to study the stall cells and their propagation velocities. The propagation velocity is where the spike stall cell can propagate through the compressor in comparison to the speed light. There are many different approaches, such as studying the study-state behavior change in the compression system. The spike stall is caused by the aerodynamic instabilities so if it is possible to control the region of separated flow (aerodynamic instability) the spike stall can be avoided [11]

There are different ways to provide solutions using measurement and control theory to measure the pressure fluctuation and predict the spike stall frequency. For instance, Hendricks and Gysling proposed a model of a small amplitude full span distributor called the stall precursor [11]. In 2006 Huu Duc Vo proposed experimental verification of the injection model as an actuator compressor injection model to allow the incorporation of the direct feedback into the operation of the system [11]. A close-loop system identification for a system under varying flow coefficients resulted in the development of an active controller to suppress the inception of modal stall. [11]. The open-loop model from the system identification resulted in the capturing the first harmonic of the fluid flow. The investigation looked at what flow coefficients are prone to cause the inception of spike stall [11]. In 1995 Paduano developed an experimental approach using Lee and Greitzer design of general mechanical construction of machine [3]. He applied the suppression modal in a single-stage low-speed axial compressor [10]. Paduano designed a feedback controller that can control the first three harmonics to discover the stall coefficient. Using the feedback controller, Panduano improved the stall margin by 23% [3]. All these different studies did develop and use experimental data of the pressure or the velocity fluctuation within the compressor. These fluctuations appeared with increasing regularity until the regime of propagating tip stall was entered. In 1988, McDougall noticed that the rotating stall at axial compressors occurs in low amplitude pre-stall conditions [5]. In 1955, S. R. Montgomery conducted research with the National Advisory Committee for Aeronautics Contract which resulted in an experiment that allowed the investigation of a single stage of an axial flow compressor [9]. The experiment was to investigate spike stall frequency by studying and measuring the spike stall cells propagation velocity. At the large mass flow rate, the number of stall cells decreased and tended to induce rotating stall [9]. S. R. Montgomery studied several theories which have been put mathematical model analyses to predict the propagation velocity of stall cells [9]. The result of S. R. Montgomery research's is the pressure fluctuations can be negligible at the downstream of the blades row; the study was made at the outer casing of the compressor [9]. The investigation developed a numerical model using fluctuations pressure and velocity to predicate spike stall frequency.

3.2 Study spike stall methods

Investigation of a rotating stall in an axial compressor using a mathematically prediction model is difficult because of its randomness. However, it is impossible to investigate the compressor instability problems under a small flow rate that causes blade fatigue. The mathematical prediction model can solve the problem of rotating spike stall. Several theories have been put forward studying spike stall causes and the relationship between solving spike stall issues in small flow rate ranges. The numerical investigation has been applied in different jet engine stages running at a low speed that is significantly restricting the operations at the inlet guide vanes [14]. The flow at the diffuser inlet is non-uniform, which is the main reason for the spike stall phenomenon. The spike stall warning method [14] proves the spike stall formation always grows in the compressor's first stage. The slow flow dynamic operation inside the compressor is the main response of spike stall formation on the jet engine stages [15]. Spike stall occurs in the tip of the rotor blade moving to the edge and causes the separation at different circumferential location [15].

Zhao Jia Yi measured the static pressure data at the tip of the blade experimentally to develop a mathematical warning method that will help avoid spike stall growth at the edge of the blade [14]. After inspecting the spike stall phenomenon inside the centrifugal compressor, Zhao Jia Yi found that when the operation was at small flow rate range the spike stall reached the frequency limit [14]. The turbomachinery process is mainly responsible for unsteady flow inside the compressor case, and the main responsible of spike stall formation . In 2015, G. Pullan developed an experiment that provides an excellent numerical simulation proving that the flow dynamic is primarily responsibility of spike stall in a gas jet engine [13]. Pullan found that as the pressure rises inside the jet engine compressor that this is associated with the formation of spike stall at the edge of the blades [13]. This stall warning method study was based on the blade passing signal method developed by Zhao Jiayiin 2018[14]. Numerical simulation provides a good solution to predict when the spike stall formation occurs on the compressor's blades and that is a good way to increase the efficiency of the jet engine. The model-based 3D URANS equation was developed to predict the process from normal running operation to unstable conditions [14].

The only location where the sensors need to be attached to detect rotating spike stall is at the leading edge of the blade tip of the first stage of the compressor within the jet engine. According to the M. Hewkin-Smith experiment, the spike stall started to develop and is created by the effects of unsteady flow inside the compressor. That is why the sensors were installed at the tip of the blade passage of the van diffuser [14]. There might be the formation of a spike stall in the middle of the blade passage of the compressor of the jet engine, but it is hard to discover because it is impossible to obtain pressure data or velocity data at these locations since no sensor can be installed there. According to M. Hewkin-Smith, one of the leading causes of spike stall is the leakage's air flow at the tip of the rotating blades and the inner casing of the compressor [16]. M. Hewkin-Smith published research about the role tip air flow leakage in creating spike stall [16]. The tip flow leakage is the extra flow which is driven through the tip clearance by the pressure difference between the pressure and suction sides of the blades [16]. The unsteady airflow passes throw the corner of the blade passage inside the compressor and is also related to the tip leakage spillage. M. Hewkin-Smith's research proposed a numerical simulation and plotted the characterization of the tip leakage flow axial momentum distribution. M. Hewkin-Smith developed a simulation using unsteady Reynold averaged Navier-Stokes (RANS) solver with the Spalart-Allmaras turbulence model [16]. Numerical simulation by GU et al. studied the effect of volute-asymmetries inside a high-pressure compressor [17]. The result proved that the relationship between the change of the velocity between the layers can affect the spike stall formation in a high-pressure compressor [Investigation of the spike stall warning method using the blade passing signal]. Developing numerical simulations to inspect the spike stall phenomenon is a good method to predict spike stall conditions, and based on the numerical simulation predications, the spike stall issue can be avoided**.** Sensors needed to be attached to the compressor to measure and record the dynamic flow properties inside the jet engine's compressor**.** Due to changes that occurred in the aerodynamic properties inside the compressor stages and based on those changes, numerical simulations have been developed over the past years**.** Many scholars have studied the compressor fan aerodynamic stability and the relationship between rotor blade tip flow and compressor the aerodynamic flow stability [18]. Aerodynamic flow stability is one of the main causes of formation of spike stall formation at the edge of the fan blades. Therefore, many scholars have tried to understand the change of the aerodynamic flow inside the compressor**.**

3.3 Numerical study experimental methods

Study of the spike stall and surge in compression system has been continuously since the early development of the gas jet engine [19]. Hoying has provided a remarkable study that includes developing a numerical method of stall inspection in a low-speed, three-stage compressor system using a 3-D model [20]. In 1999, Hoying conducted a three-dimensional (3D) computation study of the stall inspection mechanism on a low-speed compressor. Another study done by Huu Duc Vo is using a numerical method for analyzing the flow aerodynamic instability and incorporating dynamic feedback [11]. An experimental investigation of velocity data points collected from a low-speed axial compressor at the 2400 rpm running compressor measured the velocity profile at relative axial location [11]. Huu Duc Vo developed an injector model that utilized the control volume to analysis of a jet actuator [11]. Discovering the flow coefficient using open-loop system identification resulted in discovering the first harmonic and the ability to compare it with a close-loop system to help with the prediction of the instability of aerodynamic systems [11]. The goal of this thesis work is to study the dynamics of the fluid flow inside a blade passage and utilize the proposed application of the Extreme Studentized Deviate ESD test to identify precursors of stall inception for spike stall type axial compressors.

The numerical simulation control system method has been a good way to investigate spike stall that occures in jet engine compressors. The numerical simulation control system method is to approximate the stability limit of the compressor in the jet engine operation. In this work, the Idaho State University jet engine team developed a mathematical structure to accommodate the dynamic of the flow within the blade passage in order to capture any precursor development. In addition, the reported Autocorrelation method is re-created for comparison purposes. This method uses the autocorrelation of the same pressure sensor mounted at the casing of the compressor measuring the pressure of the same blade passage at each revolution. For data processing purposes, pressure data are also collected experimentally from one stage and three-stage compressors from our partner university in China. The data collection was conducted at different flow conditions, mostly close to the stall formation condition. The predication method utilizes an Autoregressive (AR) models, the extraction of the time dependent eigenvalues of the AR model, and the application of an outlier detection algorithm, called ESD tests. These methods were applied to data collected from the one-stage and three-stage compressors. The usage of autocorrelation to identify the causes of spike stall was proposed by Huu Duc Vo in 2006 [11]. The autocorrelation application models study the dynamic aspects of the spike stall conditions and develop a prediction method utilizing statistical measures of different spike stall conditions. The jet engine team proposed collecting experimental data points from an axial compressor and attaching a pressure sensor in the first stage of the eleven stages of the compressor within the Westinghouse J-34 jet engine. The team proposed to accommodate the first data collection of Westinghouse J-34 jet engine by modifying the existing setup, incorporate an electric drive system for safe operation of the jet engine at the Measurement and Control Engineering Research Center. The objective of this portion of the work detailed in this thesis is to create experimental infrastructure that allows for testing of the methods detailed in this thesis.

4.0 Chapter Four

To obtain experimental data, a partner University in China provided data from experiments designed by ISU. The data was generated using two different compressor systems: a one-stage low speed compressor and a three-stage axial compressor system. Data was collected using Kulite™ pressure sensor at high frequency (up to 20 kHz). Compressors system exhibit spike stall characteristics. Generally, rotating stall travels at 40-50% of rotating speed and the type of stall, i.e. modal stall or spike stall is a function of the blade geometry. Following Pullan G work, who developed a numerical simulation in a slow-speed one-stage jet engine compressor, this research utilizes an ESD test on the extracted eigenvalues of the respective AR models capturing the pressure response inside a blade passage. This is done for both the one stage and the three stage compressor, running at a low speed (i.e. 2,000 rpm). The data collected corresponds to the compressor operating at a flow coefficient between the range of 0.49 and 0.58, where 0.49 is indicative of operating close to stall. While the data collected with the jet engine were operating between the range of 0.49 and 0.58 flow coefficients, the average clearance between the blades tip and the sensor was 1 mm . The latter bound represents the stall point's vicinity while the experiments were carried out The parameters of the one stage axial compressor are displayed in

Table 1 One-stage axial compressor design parameters [17].

Parameter	Quantity
Design speed (rpm)	2400
Rotor blade number	60
Stator blade number	60/60/60
Outer diameter (mm)	500
Mass flow rate (kg/s)	3.2`
Rotor tip chord (mm)	36.3
Rotor tip stagger angle (deg)	39.2
Hub-tip ratio	0.75
Tip clearance / blade cord	1

the table. The three-stage axial compressor was designed to collect data with the system running in a high- compression mode and running at a low speed, similar to the one stage compressor. Like the one stage compressor, the three-stage compressor runs both experiments in low-speed axial operation with sensors attached to the casing close to the blades tip. The specific design parameters of the three-stage axial compressor are shown in the table below.

Table 2Three-stage axial compressor design parameters [17].

Parameter	Quantity
Design speed (rpm)	2400
Rotor blades number	60/60/58
Stator blade number	60/60/60
Outer diameter	500
Mass flow rate (kg/s)	3.2`
Rotor tip chord (mm)	36.3
Rotor tip stagger angle (deg)	39.2
Hub-tip ratio	0.75
Tip clearance / blade cord	2.5%

The pressure sensors utilized are set to measure the air pressure at high frequency. There are 12 sensors attached to the compressor. Sensors 1 and 12 measured flow coefficient and pressure rise, but sensors 2 to 11 were dedicated to the dynamic blades passage. The senores were attached in the clearance on the casing close to the leading edge of the blade. For the autocorrelation analysis, a set of sensors were installed at eight locations equally distributed around the circumference, as shown in Figure 1. The pressure was recorded from each run as the blades passed the sensors for each run, while the rotor speed was kept constant. The data acquisition system recorded the static and total pressures.

Figure 12 Side view of the one-stage axial compressor system [17].

Figure 11 shows the sensor location close along the blade passage, where the view was rotated 90 degrees to show the alignment of the array of sensors with the blade angle with respect to the rotating axis. Figure 12 shows sensor two at the leading edge of the compressor blade; this is a

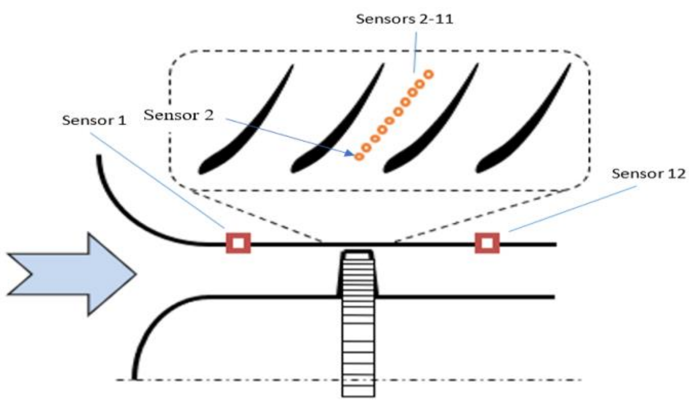

Figure 13 Sensor location for the experimental setup [17].

side view of where the sensor is located. For the three-stage compressor, the sensors were attached to each of the three-stages of the compressor, as shown in Figure 13. This three-stage compressor also used smooth casing, and data was collected at high frequency measured by Hz and the sensors were arranged as shown in Figure 13. The sensors were attached close to the blade, operating up to 18 channels for reading the pressure in each of the three stages. A sensor was also placed on level of the upstream rotor blade to record the static inlet pressure, as shown in Figure 14.

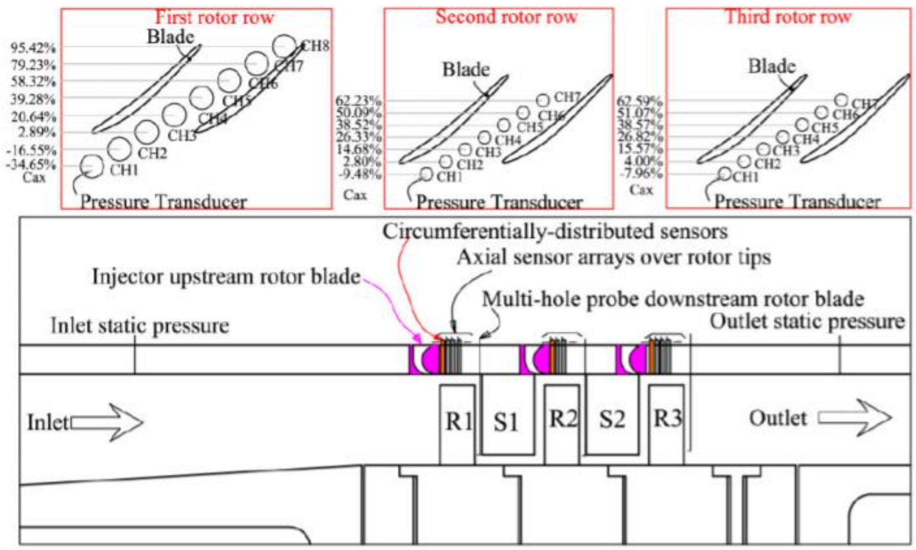

Figure 14 Sensor location for the experimental setup using the three-stage compressor [17].

To correlate the rotational speed, the individual blade passage, and the number of pressure data measured during one blade passage, a hall-effect sensor was used to recording each turn. To simulate the loading of a jet engine, and for that matter the loading of the compressor, a throttle valve is used at the exhaust of the compressor. This makes it possible to maneuvering the operating point of the compressor to different a flow coefficient, including near stall inception.

4.1 Mathematical description

4.1.1 Build numerical simulation for data grouping

Using pressure data collected from both the single-stage and the three-stages compressor, an autoregressive (AR) model is extracted to study the changes in the pressure of the fluid behavior between the blade passages of a compressor stages. After collecting the pressure data points under different conditions and running situation in the compressor for cases where stall occurred but also for cases where no stall occurred, the pressure data points were grouped using an algorithm called the sliding window algorithm.

1. Sliding Window Algorithm

The sliding window algorithm is a sub-list that runs over an underlying collection of data points and computes the running average. The sliding window algorithm is used to solve problems that involved an array and reduce time complexity. In this work, it is used to prepare a data group of data points to extract an AR model as well as to track the autocorrelation of pressure data between one full turn at a time. The sliding window algorithm is defined by the number of data points n and sliding window length *w*. The result of n-w is the total number of data groups that will be used for the proposed and comparison algorithms. The autocorrelation is a mathematical methodology which represents the degree of similarity between a lagged version and time series over successive time intervals. The sliding window algorithm is used for the autocorrelation computation of the pressure data collected during one pass of one blade passage and correlated with the data one revolution ago.

$$r_k = \frac{\sum_{t=k+1}^{n}(y_t - \bar{y})(y_{t-k} - \overline{y)}}{\sum_{t=1}^{n}(y_t - \bar{\bar{y}})^2}$$

4.1.2 Data grouping numerically

The objective of the autocorrelation method is to take the average of each data set representing one blade passage related to the same blade passing by one revolution later and observe its drift. The drift is computed by grouping a set of autocorrelation data points and using a sliding window algorithm. Another grouping algorithm is employed for the proposed ESD method, where the data is grouped by an increasing length of window size. This method is called the growing window algorithm. In general, correlation changes the data pattern from not apparent pattern to defined pattern and takes the average of the data points. The growing window algorithm is a numerical technique which also uses sequential data grouping method and to prepare data samples for the ESD test. To define the number of the outliers in the data, the upper bound of the outlier needed to be defined is currently set arbitrarily. The data points in the growing window algorithm use the ESD to linearize the growth rate. The number of the data point n and has a window length w which allows for the computation of the growth rate g, i.e. the total number of data group that result. To develop a rotating stall inception indicator for a multistage compressor, a mathematical model is needed. In this work, two approaches are utilized to detect spike stall: one is the statistical method using autocorrelation of pressure data, and the second is the generalized extreme studentized deviation for the moving window algorithm model. Using MATLAB™'s implementation for computing the correlation coefficient , the sliding window algorithm is utilized to capture the trend of over time of the correlation flow coefficient. The goal of applying the ESD test on the grouped data is to detect the outlier of the eigenvalues of the extracted AR models.

4.2 Mathematical model

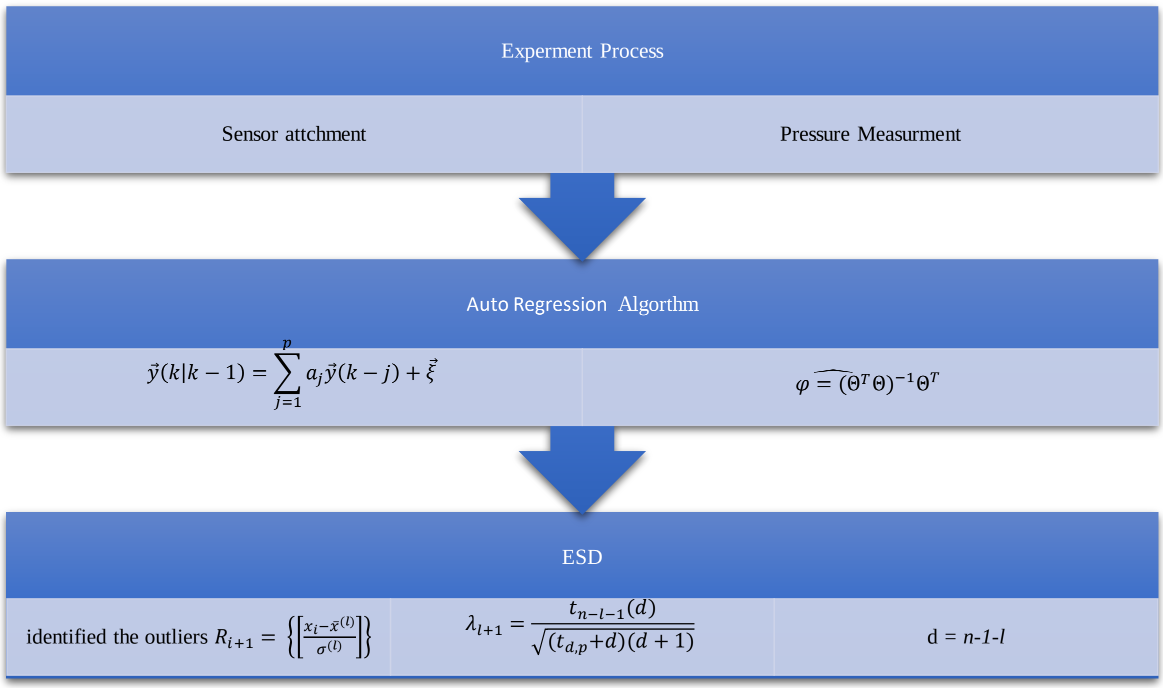

4.3 Growing Window Algorithm

The growing window algorithm is used to group the pressure data set which is obtained from sensor No. 2 as indicated in Figure 14 This sensor is the leading sensor at the blade passage's tip. It is used to prepare the data samples for the ESD test. The window growth rate is linear. Assuming n is the total number of the data groups, and w is the initial window size, then the growth rate is g, so the total number of the data grouped is n.

$$\frac{n-w}{g} + 1$$

4.3.1 Auto Regression

To predict when spike stall occurs, autoregression of the pressure data is a good method that can be used to observe the pressure data fluctuation occurring in one particular blade passage over time. The ESD and the autoregression method are both statistical approaches and they do not incorporate any mathematical structure to accommodate the dynamic of the stall formation [16].

To indicate spike stall dynamic development, a time series model is not important for predication. For spike stall investigation, the autoregressive model is proposed for the use of spike stall prediction, [16]. The AR model can accommodate the stall formation indicators which are represented by sharp changes in the dynamic description of the AR model. The sudden changes of the dynamics are detected by using an outlier algorithm, i.e. the ESD test on the eigenvalues of the AR model. The AR model was extracted from the data received from the leading-edge sensor at different flow coefficient. In this project, the AR model was proposed to use the embedded dynamic representations to model a time series to predict spike stall dynamic.

$$\vec{y}(k|k-1) = \sum_{j=1}^{p} a_j \vec{y}(k-j) + \vec{\xi}$$

Let $\vec{y}$ be the collected pressure data, then k is assumed the time index, and the coefficient matrices are the tap weights of this filter, while $\vec{\xi}$ is the residual. The estimation of the coefficient matrices can be done recursively using data matrix as define by the equation below, where L is the current

$$\Theta_{k+1} = \begin{bmatrix} \overrightarrow{y_p^T} & \overrightarrow{y_{p-1}^T} & \overrightarrow{y_{p-2}^T} & \cdots & \overrightarrow{y_1^T} \\ \overrightarrow{y_{p+1}^T} & \overrightarrow{y_p^T} & \overrightarrow{y_{p-1}^T} & & \overrightarrow{y_2^T} \\ \vdots & \vdots & \vdots & \cdots & \vdots \\ \overrightarrow{y_{L-1}^T} & \overrightarrow{y_{L-2}^T} & \vec{y}_{L-3}^T & \cdots & \overrightarrow{y_{L-p-1}^T} \\ \vec{y}_L^T & \vec{y}_{L-1}^T & \vec{y}_{L-2}^T & & \overrightarrow{y_{L-p}^T} \end{bmatrix} = \left[\frac{\Theta_k}{\phi_{k+1}}\right],$$

length of the matrix as it is shown in the equation above. A new row vector is added to the data matrix, given by Θ_{k+1}. Then the inverse covariance matrix P_k at the time k and can be used to construct a recursive method, this is detailed in reference [24]. This formula is the recursive formula, and it is used to estimate the AR coefficient.

$$P_{k+1} = P_k \vec{\phi}_{k+1}^T \frac{\vec{\phi}_{k+1}^T P_k}{1 + \vec{\phi}_{k+1}^T P_k \vec{\phi}_{k+1}^T}$$

Using this equation, the parameter estimate can be defined using the estimation vectors $\varphi_k = [a_1 a_2 \dots \dots a_p]$ and the updated estimation can be calculated using $\hat{\varphi} = (\Theta^T \Theta)^{-1} \Theta^T \vec{\varepsilon}$ and to calculate $\vec{\varepsilon} = [\vec{y}_{p+1} \vec{y}_{p+2} \dots \dots . \vec{y}_L]$. The canonical realization was used to extract the embedded dynamic by realizing a state-space form of the AR model, which can be written as

$$\vec{y}(k|k-1) = \begin{bmatrix} \vec{y}_k \\ \vec{y}_{k-1} \\ \vec{y}_{k-2} \\ \vdots \\ \vec{y}_{k-p+1} \end{bmatrix} = \begin{bmatrix} a_1 & a_1 & a_1 & \cdots & a_1 \\ 1 & 0 & 0 & \dots & 0 \\ 0 & 1 & 0 & \ddots & 0 \\ \vdots & \vdots & \vdots & \vdots & \vdots \\ 0 & 0 & 0 & \dots & 0 \end{bmatrix} \begin{bmatrix} \vec{y}_{k-1} \\ \vec{y}_{k-2} \\ \vec{y}_{k-3} \\ \vdots \\ \vec{y}_{k-p} \end{bmatrix} + \begin{bmatrix} \vec{\xi}_k \\ 0 \\ 0 \\ 0 \\ 0 \end{bmatrix}$$

This equation can be written as an $\hat{\varphi}$ system matrix $\hat{\varphi} = \Theta^T \lambda\ \Theta$, where Θ is the eigenvector and λ is the eigenvalue. The eigenvalues can be plotted and tested using the ESD test to indicate the spike stall formation in pressure data which was measured at the tip of the leading edge.

4.3.2 Autocorrelation

The data need to be grouped based on data points per revolution in order to apply the autocorrelation on the grouped data. The average number of data points per passage of one blade section is grouped by using the sliding window algorithm. To correlate between the two windows the Person correlation coefficient utilizing *MATLAB*®'s implementation is applied.

4.3.3 Generalized Extreme Studentized test

After grouping data using the growing window algorithm, the ESD test is used in conjunction with the growing window to detect the outliers. The autocorrelation method is used to find the outliers from the data points so the outliers could be tested using the ESD test. An outlier is an extremely large value or an extremely small value of the data points; this means it is the unusual point in the data set. To identify the outliers among the data, a point must satisfy a specific criteria: it must be greater than $a_3 + 1.5(IQR)$ or less than $a_4 - 1.5(IQR)$. The $a_3 + 1.5(IQR)$ is to identify the outliers of the data grouped, *QR* is the data groped under the third quarter or above the third quarter. This result in an interquartile range of acceptable data and identified outliers [21]. The ESD test allows one to observe the dynamic of the outliers. The generalized ESD test is very useful because the number of outliers here is unknown. The outliers has an upper bound *k* which in this study is arbitrary defined for the number of maximum outliers of each eigenvalue. The mean and standard deviation of the data sample is calculated first. The growing window algorithm is then used to inspect spike stall by comparing the outliers' eigenvalues. When the calculation shows an increasing trend of the number of outliers detected, spike stall inception is associated with this occurrence. To develop an ESD test, these steps are performed on the data set.

1. The ESD methods identified the outliers by calculating interquartile range and the maximum outlier present R_{i+1} for which $l = 0 \ldots . k - l$.

$$R_{i+1} = \left\{ \left[\frac{x_i - \bar{x}^{(l)}}{\sigma^{(l)}} \right] \right\}$$

2. The critical value λ_l was calculated as well as the extreme large value and the extreme small value in order to compare to data point to find the outliers.

$$\lambda_{l+1} = \frac{t_{n-l-1}(d)}{\sqrt{(t_{d,p} + d)(d+1)}}$$

   The percentile was represented by *t* for t-distribution as $p = 1 - \frac{a}{d+1}$ for specific number of degrees of freedom *d* and *d* was calculated $d = n - 1 - l$.

3. The confidence level in this application is calculated to be $\alpha = 0.05$ and then the value of *t* was identified and determined by calculate the percentile p for specific number of degrees of freedom or d.

4. After grouping all the data and finding the outliers, the other data grouped were removed to reduce the size of matrix by removing the data group R_l.
5. The maximum number of the outliers was added to the upper bound of the outlier k; therefore, the next step is important.
6. Steps 1 to 4 needed to be run in a loop until maximum number of the outlier was removed from the data group.
7. The remaining number of data points in the data group was the maximum number of outlier k; it had to be less than the original number of data points. The actual number of outliers was defined as the upper bound of outliers determined. The maximum number of outliers after the ESD test achieved the following condition.

The growing window algorithm needed to be used to build up the main matrix to use the ESD test, generating a matrix of specific size. For every window, the nested loops involved with the ever-increasing windows' length grew at a particular growth rate. The number of outliers was plotted representing revolutions per the eigenvalue.

4.4 Idaho State University Jet Engine Sensor System

At Idaho State University, the jet engine team started to modify a setup in order to collect pressure data from a Westinghouse J-34 jet engine. The 1957 jet engine runs on gas and has a gearbox that transmits power from the engine rotor to the accessories. The J34 WE-36 has eleven stages in the compressor section, which is shown in the Figure 15. The compressor assembly consists of a shaft and two stages 1st stage wheel and 2nd stage wheel bolted together by two sets of bolts. The compressor is located between the first bearing and the combustion chamber and consist of a rotor assembly and a compressor vane outlet assembly.

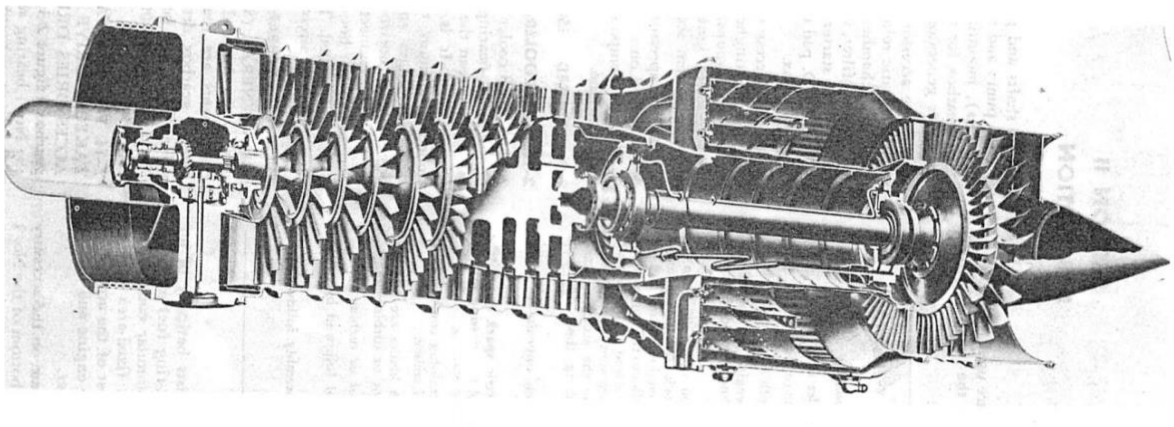

Figure 15 Jet engine J34 WE-36 [4].

The Westinghouse J-34 jet engine is on permanent load to the Measurement and Control Engineering Research Center (MCERC) for the purpose of conducting research in stall detection, fault analysis, fault prediction, dynamic modeling, flow analysis, control system design, estimation, and modelling using machine learning methods. For these purposes a data collection system to measure pressure at high frequency is required. For this purpose, instead of running the jet engine on gas, a senior design team designed an electrical motor system to run the jet compressor. It was attached to a table that had been designed to observe vibration during the running operation of the jet engine compressor as shown in Figure 16. The jet compressor running table was built with 36 square steel beams and one steel plate as it is as showing in Figure 19. The electrical running system was attached to the steel table. The system was consisting of an electrical motor type General Electric model number 5K215SC205 which had 9” pulley connected to the shaft of the motor as shown in figure. The second compound was a shaft with two pulleys attached, also designed by the jet engine senior design project team. The J34 WE-36 engine was an 11 stages compressor consisting

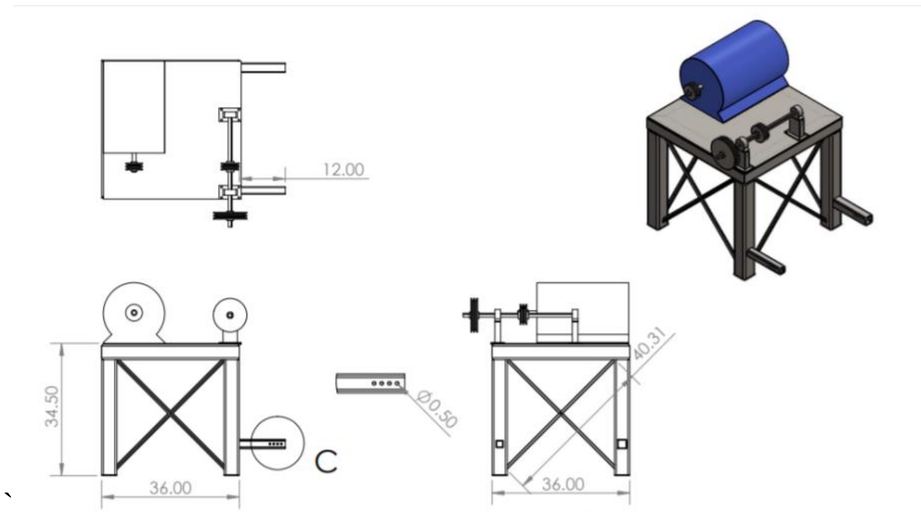

Figure 16 Electrical motor system design.

basically, of an axial flow and double annular combustion chamber with two ring fuel manifolds with 60 spray nozzles. The engine is a two-stages gas jet engine machine with a fixed- area exhaust nozzle and various accessories. The two-pulley shaft was mounted on the top of the table with four 5/8” bolts as it is shown in Figure 17. The jet engine electrical motor system rans with one shaft and two 9” pulleys and two 3” pulleys. The shaft was built with two pulleys one which was small pulley driven by the motor pulley with belt the second pulley is a 9” pulley which drove the 3” that pulley attach to the flange rotating the jet turbine nozzle. The nozzle was driven by the flange which had pulley size 3” diameter pulley which was attached to electrical running system with belt. The flange was designed by an undergraduate senior design student; the

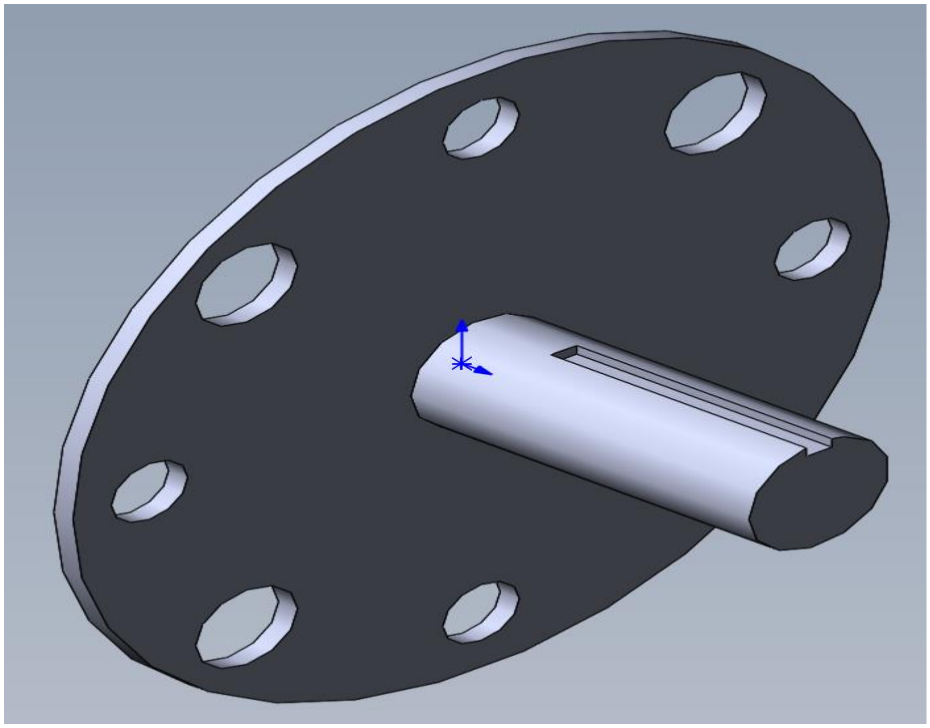

Figure 17 Flange design.

flange was attached to the power take-off gearbox by the holding fixture. This drove the shaft of the jet turbine with the electrical motor system. The flange has a pulley that connects to a small pulley of the electrical motor system using a belt as shown in Figure 18. A 10 hp General Electric motor, model number 5K215SC205, is used as the main motor. It runs using 230 to 460 volts. The motor runs in 3 phases with 60- frequency, shaft Figure 18 designed with two pulleys one is small pulley and the other bigger with a 9” diameter. The small pulley was driven by the belt attached to big pully on the motor to drive the drive shaft which had a second big pulley attached to it to drive the flange as shown in Figure 17 to run the motor. The system is attached to the steel table

Figure 18 Transmission shaft.

with four size 5/8” bolts, as it is shown in Figure 19. The future work in for the project is to attached this to the jet engine and start to operate for data collection and to calculate precursor algorithms using the experimental pressure data at different jet engine operating conditions. The sensor will be attached close to the leading edge of the compressor blade and the location needs to be calculated. To attach the sensor a 3-D print attachment model is needed to be design based on the specification of the hole in the casing of the compressor.

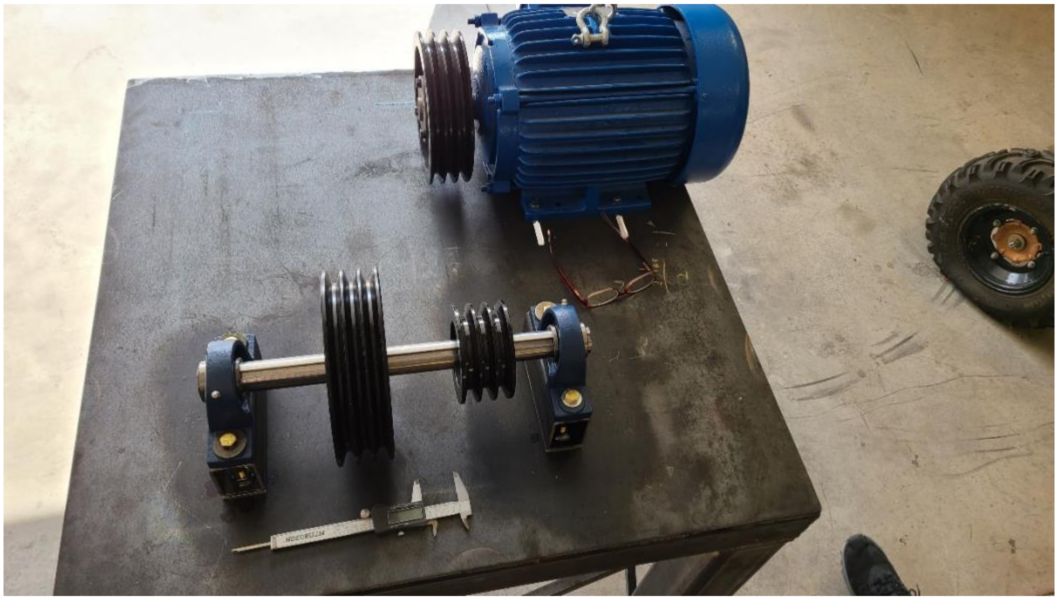

Figure 19 Electric motor system

5.0 Chapter Five

5.1 Results

Sensor 2 captures the most dynamics of the fluid flow and that is why it was chosen for the analysis. The jet turbine compressor was running at 2,400 rpm and each experiment generated 460,00 total data points that is used for the different approaches and analysis. The flow coefficient in this operation was found to be 0.505 and it is close from stall formation. To investigate the spike stall formation, a comparison between an eigenvalue of two operation of jet engine compressor is performed. The first pressure data was collected at regular operation of the compressor where no spike stall occurs. The second operation of the compressor ended up close to have spike stall formation. The comparison between two data sets was based on the behavior of eigenvalues of the pressure data.

5.2 Autocorrelation

The autocorrelation method was applied on the two data sets . The results of the correlation coefficient indicate that the flow remains *relatively consistent until around 620 revolutions, as shown in the Figure 20. At that point in time, the correlation coefficient decreases significantly. Around this revolution where the correlation coefficient drops down the formation of spike stall started in the three-stage compressor.

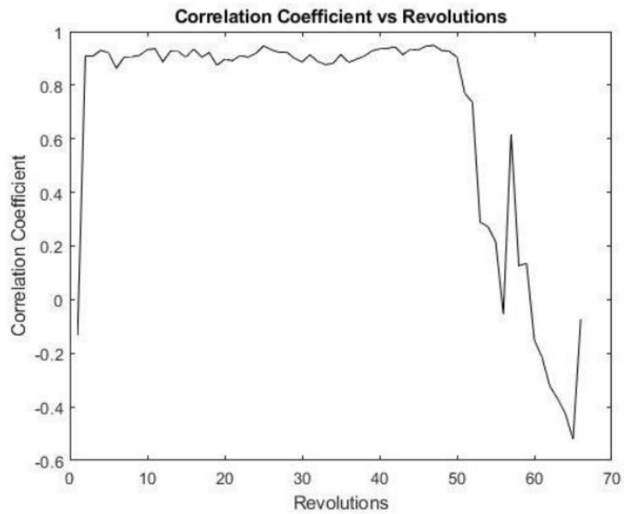

Figure 20 Autocorrelation plot for pressure data vs flow coefficient [17].

5.4 Autoregression Result

Computational time is not a focus of this work, but for this application of predication it was very useful. The pressure data was collected at condition where spike stall may occur. The data is filtered and used to test the autoregression based approach by computing the eigenvalues of the AR model. These values are plotted against the revolutions and observed for large variation, i.e. to indicate if spike stall has occurred. The pressure data points set was measured using a sensor with sampling rate of high frequency and the jet turbine compressor was operating at 2400 rpm at flow coefficient of 0.46, and 0.55. The average number of points of the stall data passing the sensor for one blade passage was found to be 2461. The pressure data points were collected at the tip of the leading edge of the blades. The data indicated that stall occurs at around 620 revolution. For the first par, the modelling of the Autoregressive model (AR), an order of 14 yielded the most promising results. In the following the 14 eigenvalues are graphically depicted as a time series plot. Note, these eigenvalues indicate stability by having an absolute magnitude of less than one (excluding 1.0). Changes in the trend of the magnitude would indicate changes of the dynamics of the flow system. The time axis, for convenience, is converted into revolutions. Figure 21 depicts the raw pressure data, where at about 2.8 x 105 revolution, stall is indicated by large variations of the pressure data. This instant in time is compared to the eigenvalues of the extracted AR model in order to deduce if predictions can be made of the onset of stall.

Comparing each plot with the indicated onset of stall as shown in Figure 21, some eigenvalues exhibit larger variation over time than others. Several the eigenvalues, such as 1, 2, 5, 7, 9, 11, and 13, reach magnitude values above 1 prior to stall. One can stipulate that these eigenvalues, and the time they occur are associated with precursors of stall formation. However, these instances also could be related to data outliers such as influence of noise and poor modelling. Hence, an outlier detection algorithm is needed prior to making any assumption of precursor indication. Also, of note to the given plot is the fact that the set of eigenvalues which depict outliers is not unique to the data set acquired from the experiment. Each processing and extraction of the data may yield a different set of eigenvalues exhibiting this behavior. It is assumed that this is related to the fact that any information on the physical coordinates is lost in the computation of these models and their eigenvalues. As stated, the purpose is to test if any of those large changes in eigenvalues is

of significance and hence possible to be associated with a precursor to stall inception. There are two types of data sets; both of them were collected from the three stage compressors. One data set is a stall data type, and it has 46,000*12 pressure data points, as shown in Figure 21 (b). The second type of pressure data that was tested is non-stall data, and it has 22,000*12 pressure data points, as shown in Figure 21 (a). The spike stall pressure data's behavior starts to change at a specific revolution, as shown in Figure 21 (a), and that is where the spike stall occurs, as shown in Figure 21 (b). These two plots can show which pressure data collected had a stall.

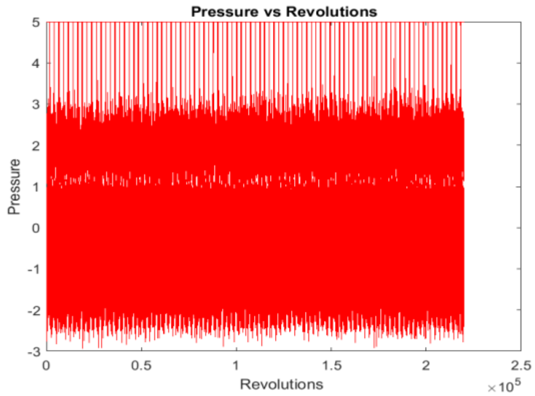

(a)

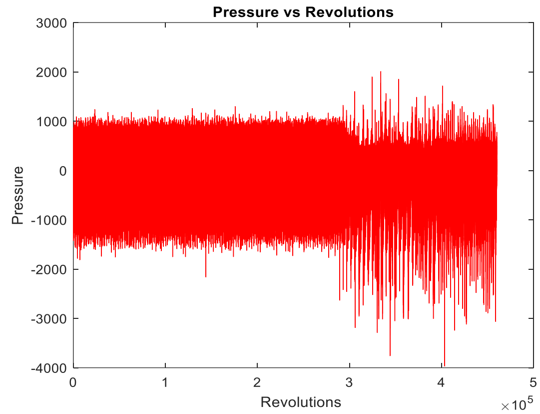

(b)

Figure 21 stall data Pressure Vs Revolutions

The autoregression model was then applied to both pressure data sets to check if the spike stall was happening at the indicated time location. The following figures show the 14 eigenvalues of the extracted AR model, corresponding to the data shown in Figure 21 (b). This data was close to stall, and the figures on the left are for pressure data in Figure 21 (a). The figures on the right side are related to non-stall data. All the 14 eigenvalues were behaving almost the same, and none of the 14 eigenvalues crossed the value of 1.0, indicating instability. However, the figures on the left side are related to the pressure data of Figure 21 (b). Each eigenvalue started to behave differently when the spike stall close to happen in the flow inside the compressor. The eigenvalues 1, 2, 5, 7, 9, 11, and 13 are the ones that cross the value of 1.0 (excluding 1.0) as shown in the Figures 22, 23, 26, 28, 31, and 33 and they are the ones that might have stall close to happening in the compressor operation.

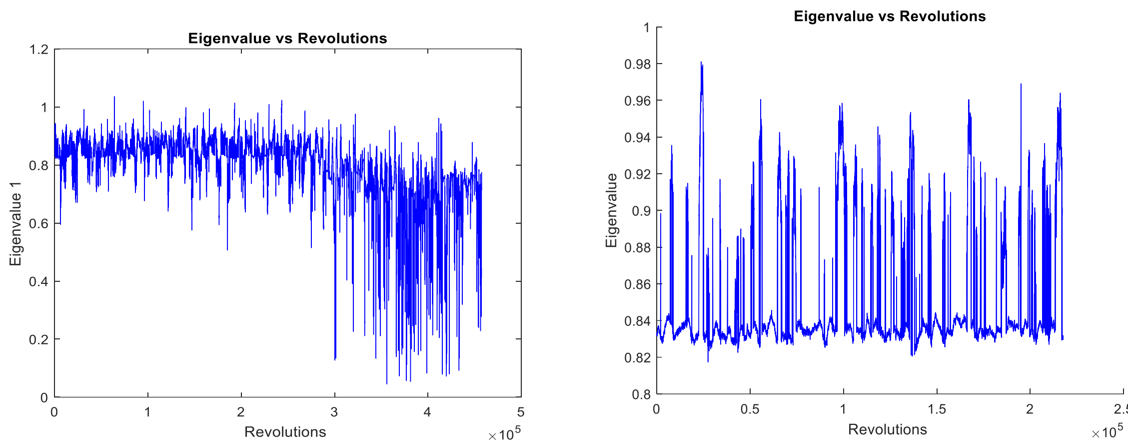

Figure 22 First eigenvalue of AR System.

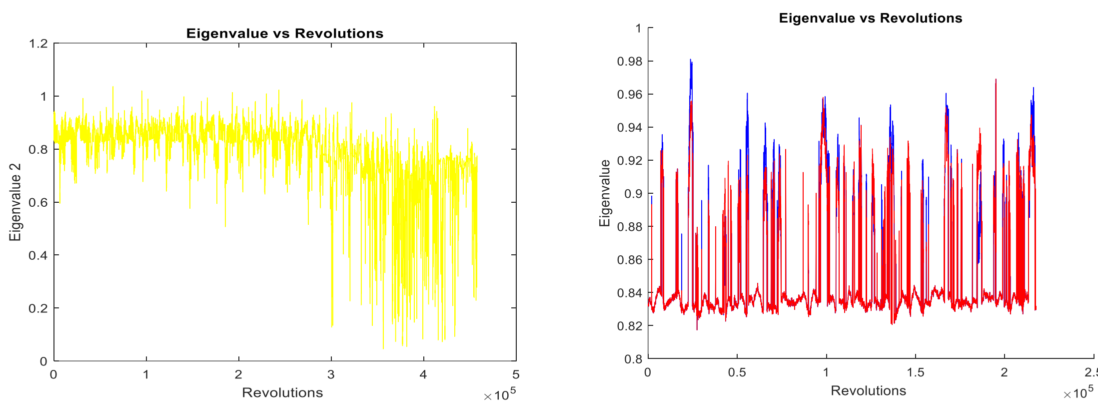

Figure 23 Second eigenvalue of AR System

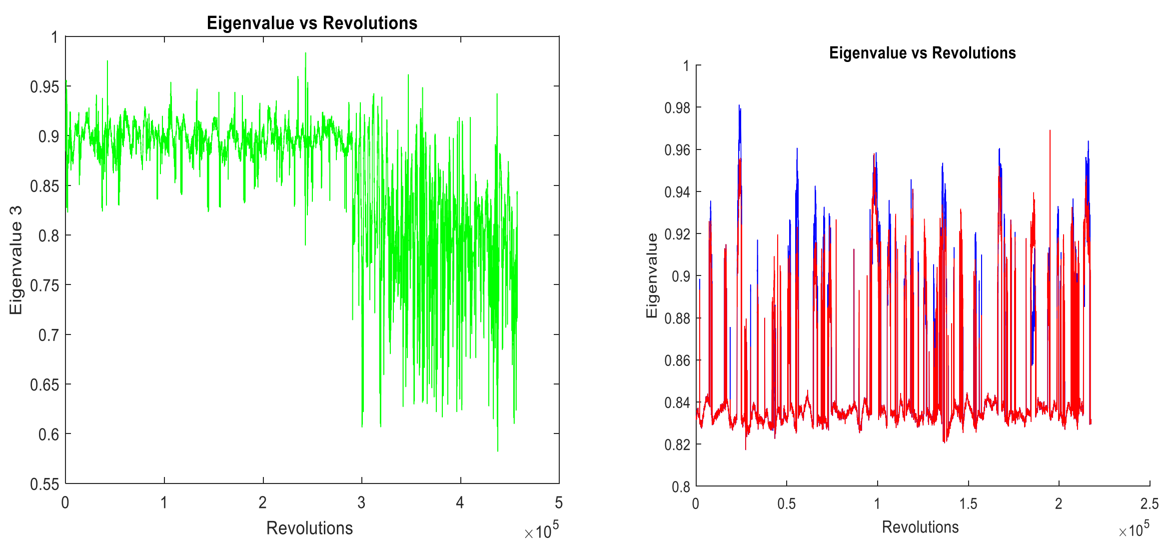

Figure 24 Third eigenvalue of AR System

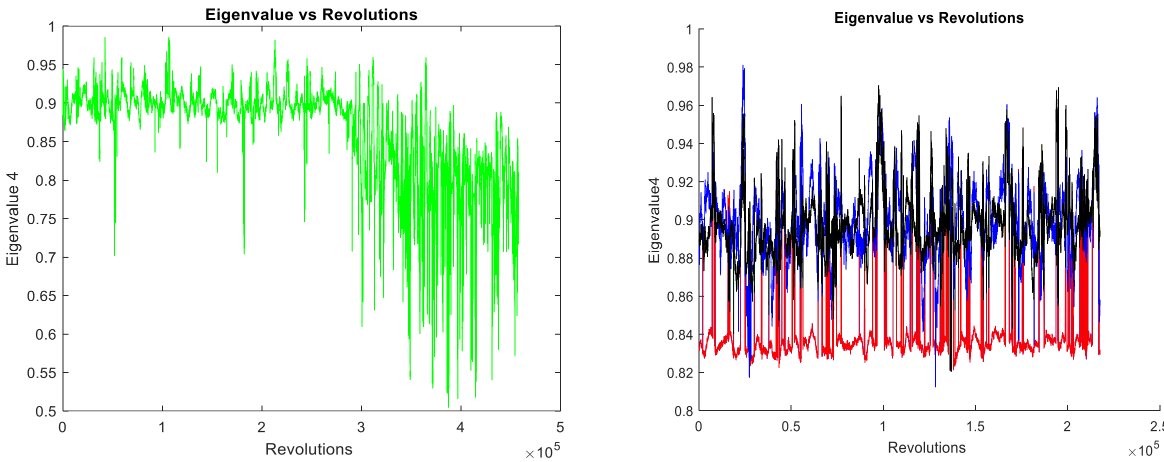

Figure 25 4th eigenvalue of AR System

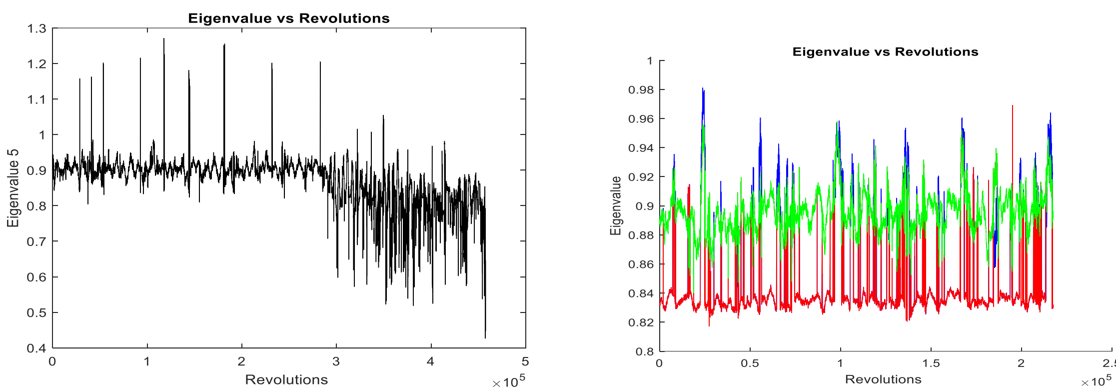

Figure 26 5th eigenvalue of AR System

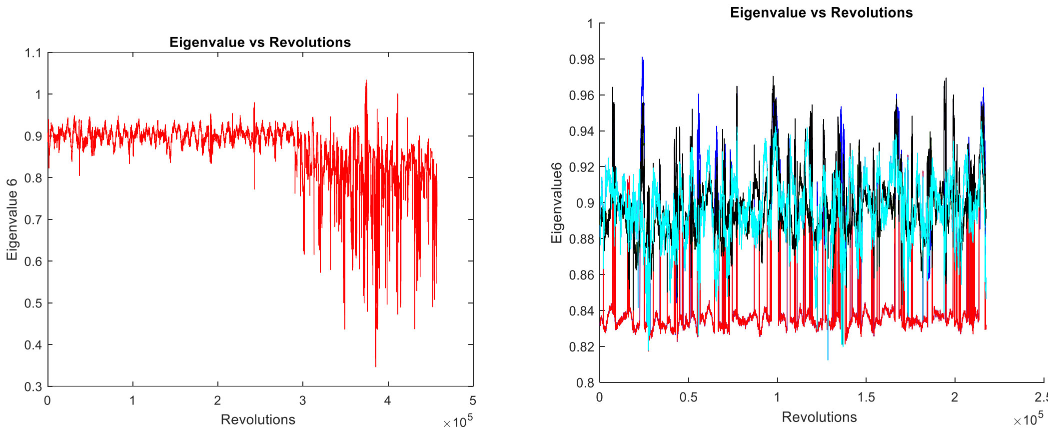

Figure 27 6th eigenvalue of AR System

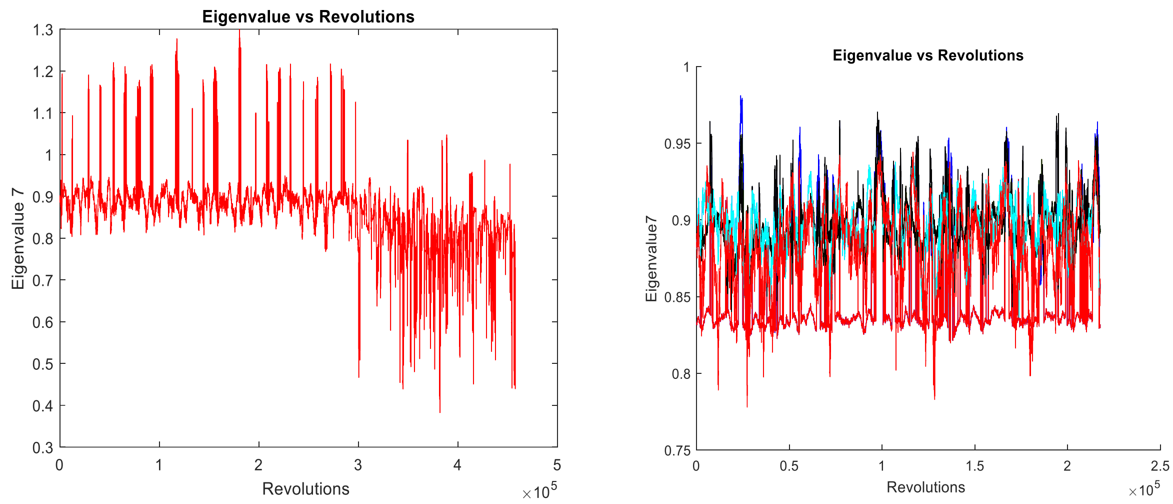

Figure 28 7th eigenvalue of AR System

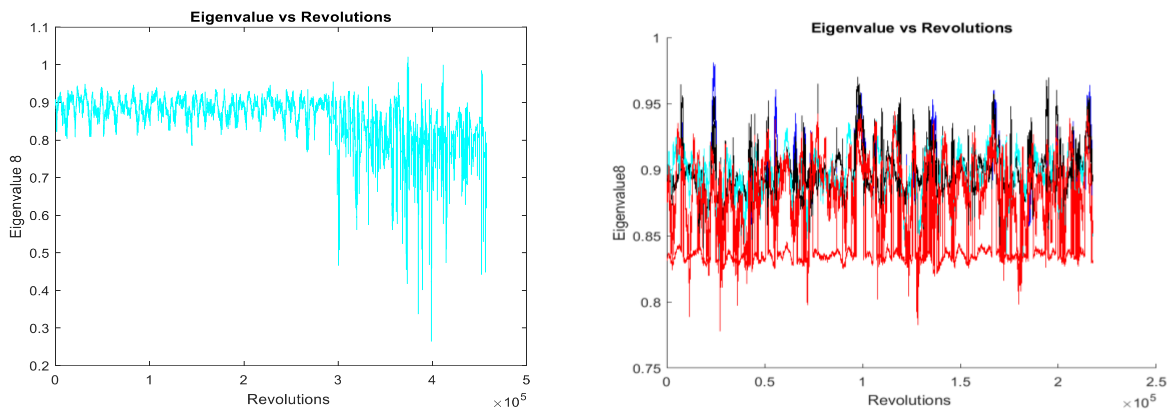

Figure 29 8th eigenvalue of AR System

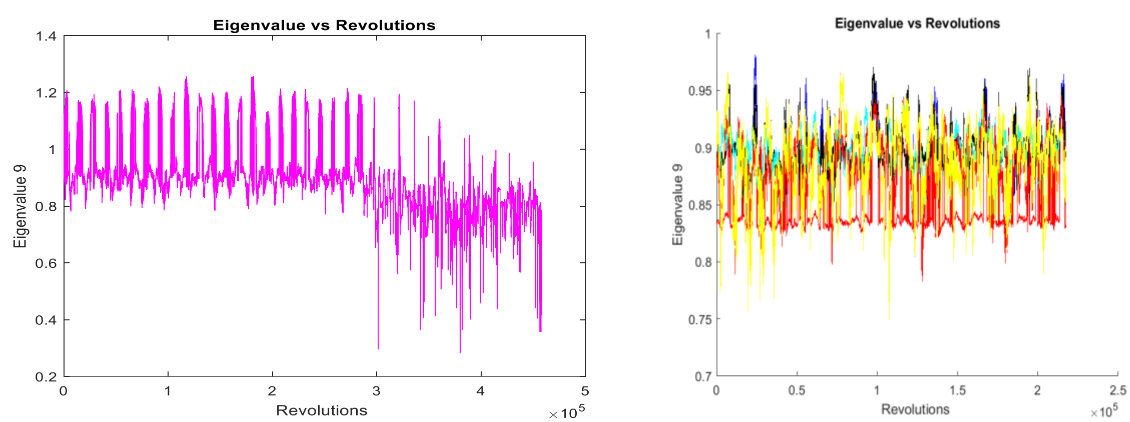

Figure 30 9th eigenvalue of AR System

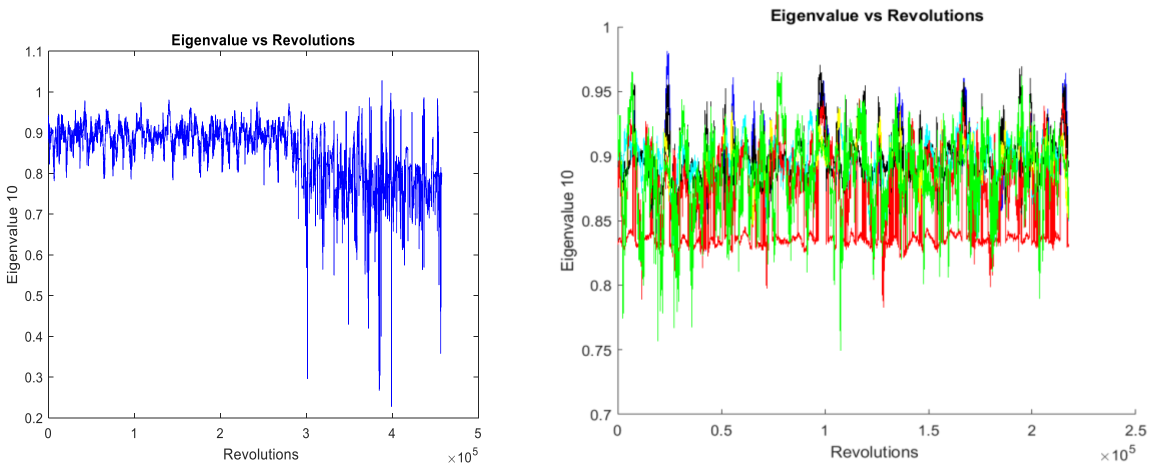

Figure 31 10th eigenvalue of AR System

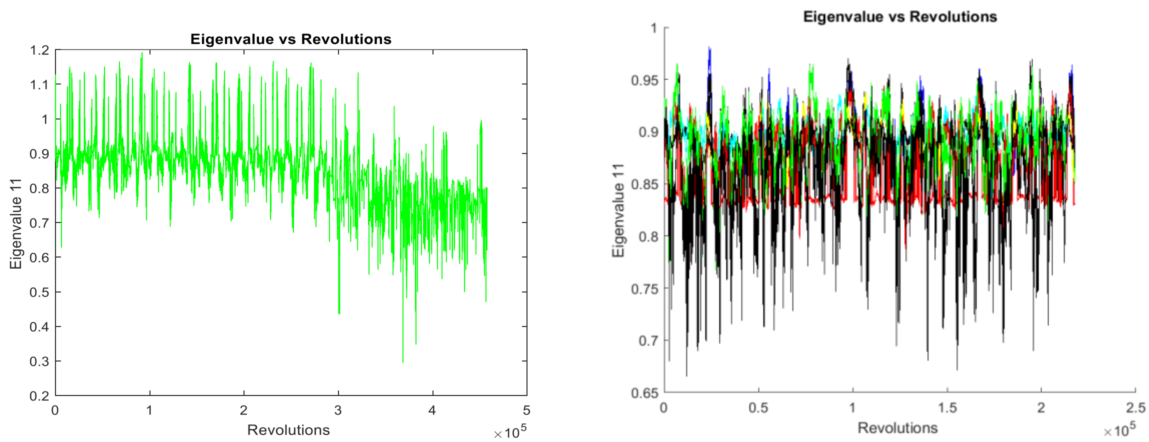

Figure 32 11th eigenvalue of AR System

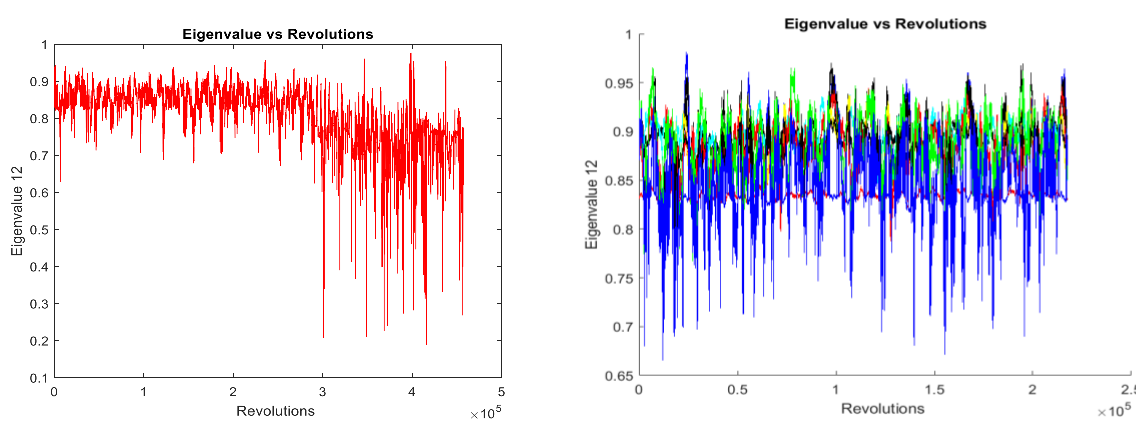

Figure 33 12th eigenvalue of AR System

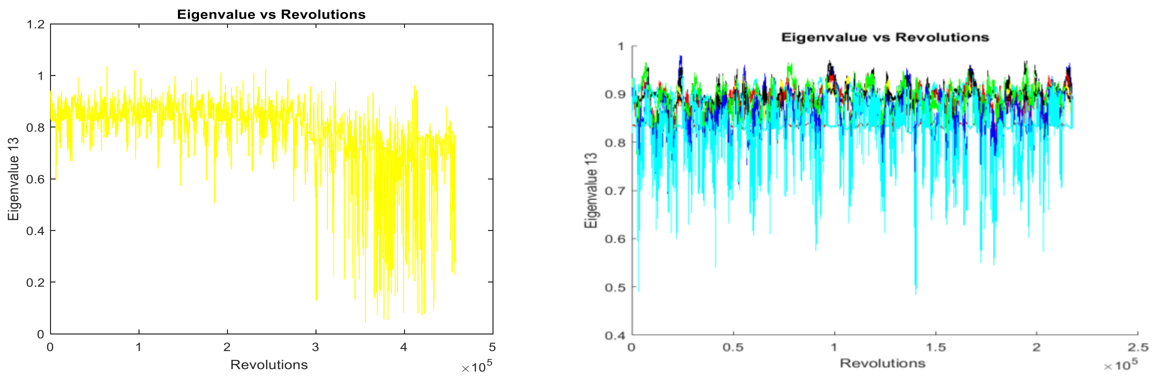

Figure 34 13th eigenvalue of AR System

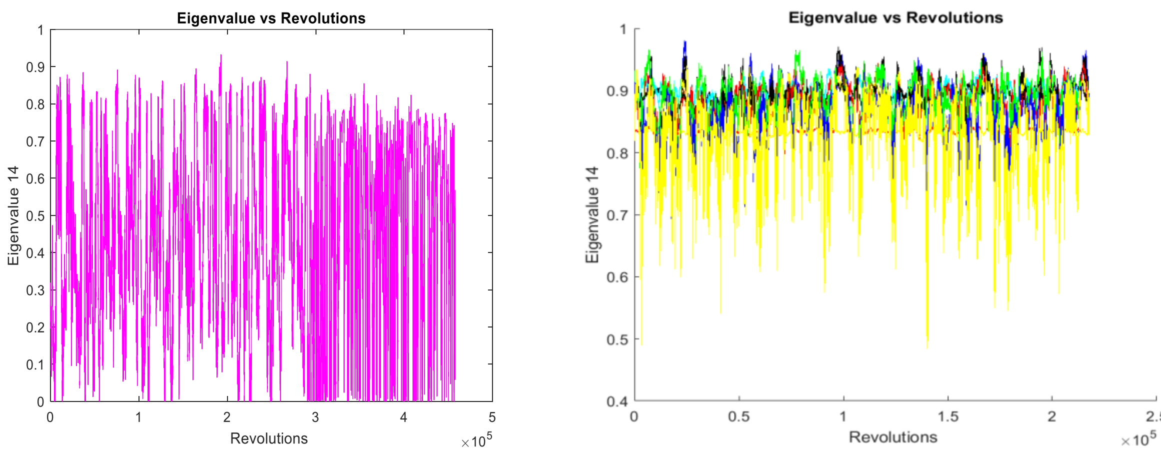

Figure 35 14th eigenvalue of AR System

5.4 ESD Result

The pressure data points set was measured using a sensor with sampling rate of high frequency and the jet turbine compressor was operating at 2,400 rpm at flow coefficient of 0.46, and 0.55. The average number of points of the stall data passing the sensor for one blade passage was found to be 2,461. The pressure data points were collected at the tip of the leading edge of the blades. The data indicated that stall occurs at around 620 revolution. For the first par, the modelling of the Autoregressive model (AR), an order of 14 yielded the most promising results. In the following the 14 eigenvalues are graphically depicted as a time series plot. Note, these eigenvalues indicate stability by having an absolute magnitude of less than one (excluding 1.0). Changes in the trend of the magnitude would indicate changes of the dynamics of the flow system. The time axis, for convenience, is converted into revolutions. Figure 36 depicts the raw pressure data, where at about 2.8 x 105 revolution, stall is indicated by large variations of the pressure data. This instant in time is compared to the eigenvalues of the extracted AR model in order to deduce if predictions can be made of the onset of stall.

Comparing each plot with the indicated onset of stall as shown in Figure 36, some eigenvalues exhibit larger variation over time than others. A number of the eigenvalues, such as 1, 2, 5, 7, 9, 11, and 13, reach magnitude values above 1 prior to stall. One can stipulate that these eigenvalues, and the time they occur are associated with precursors of stall formation. However, these instances also could be related to data outliers such as influence of noise and poor modelling. Hence, an outlier detection algorithm is needed prior to making any assumption of precursor indication. Also, of note to the given plot is the fact that the set of eigenvalues which depict outliers is not unique to the data set acquired from the experiment. Each processing and extraction of the data may yield a different set of eigenvalues exhibiting this behavior. It is assumed that this is related to the fact that any information on the physical coordinates is lost in the computation of these models and their eigenvalues.

In the following, the ESD algorithm results applied to the presented eigenvalue time history are presented. As stated, the purpose is to test if any of those massive changes in eigenvalues. Also, the eigenvalue change is hence possible to be associated with a precursor to stall inception. After specifying the eigenvalues that indicate spike stall close be format in the jet engine's compressor operation, the revolution needed to be investigated. The main two reasons for the ESD test are first is to prove the spike stall is close to happened or not. The second reason, which is more important than the first one since the spike stall formation was proved already, is to find out which revolution the spike stall is closed to happen. The ESD test indicated the spike stall occurs at around 620 revolutions, as shown in the 1, 2, 5, 7, 9, 11, and 13 eigenvalues ESD test for the outlier figures. Figure 36 (a) shows the spile stall pressure data set after filtration and prove the spike stall is close to occurs at around 620 revolutions. Figure 36 (b) is for data has no spike stall issues close to happening in the operation

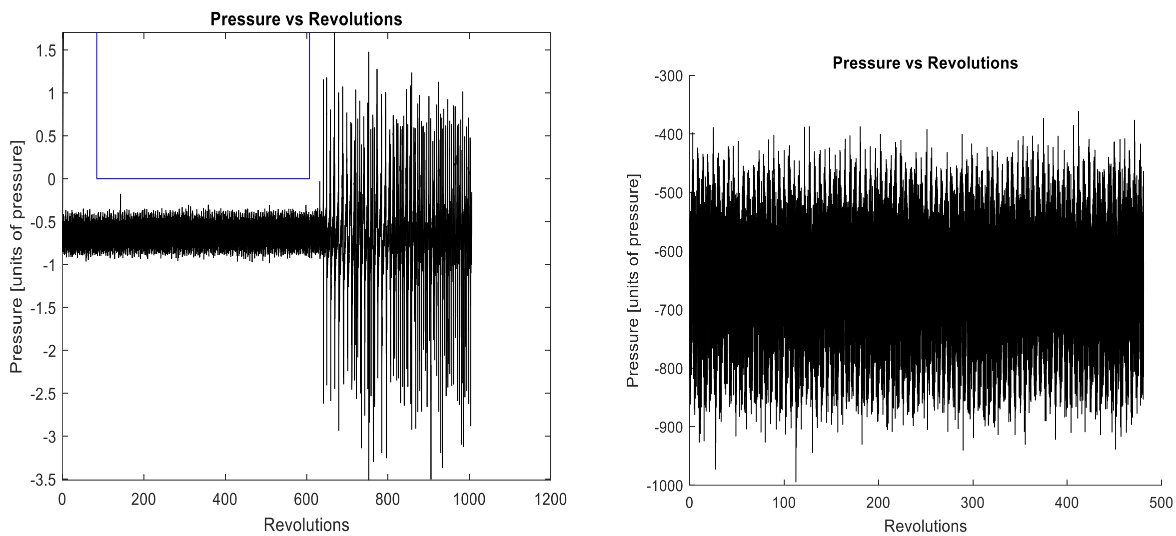

(a) *(b)*

Figure 36 Pressure vs Revolution filtered.

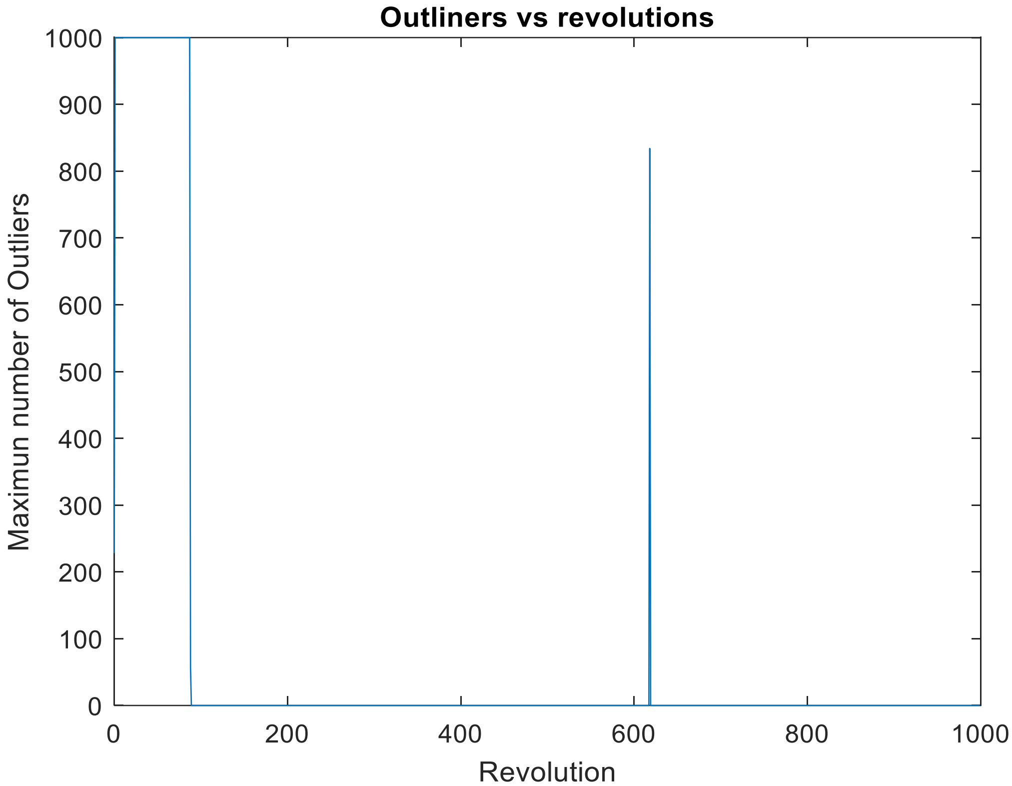

Figure 37 First eigenvalue of ESD model.

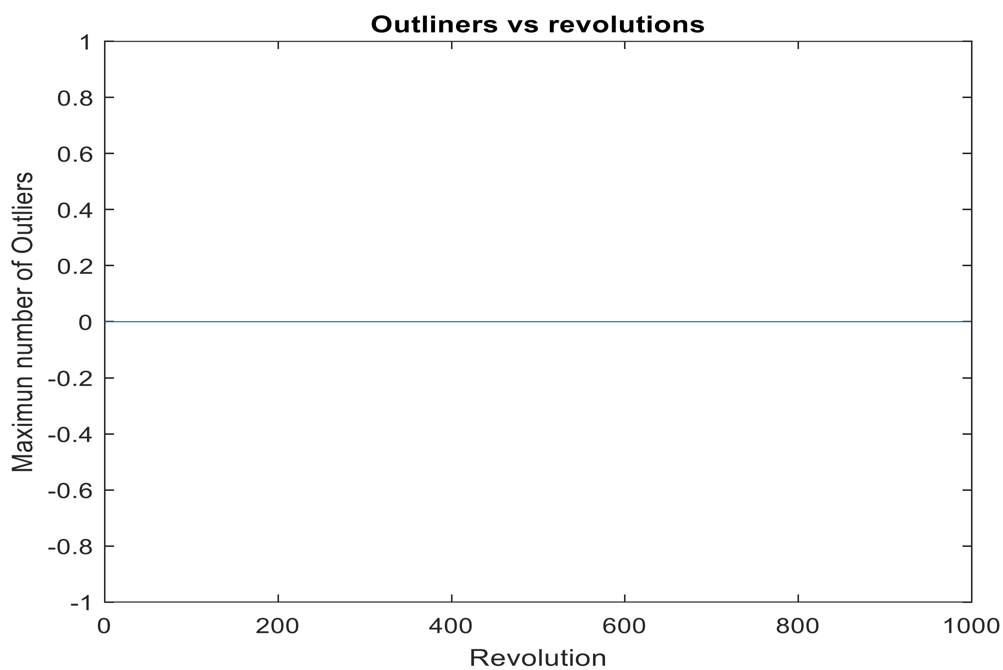

Figure 38 Second eigenvalue of ESD model.

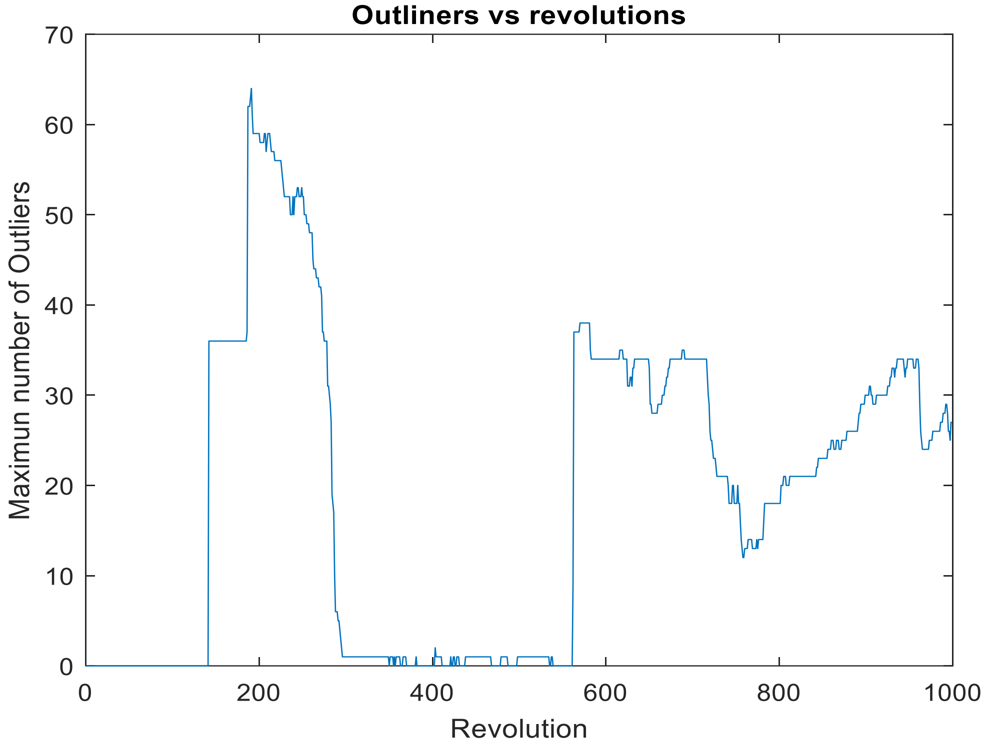

Figure 39 Third eigenvalue of ESD model.

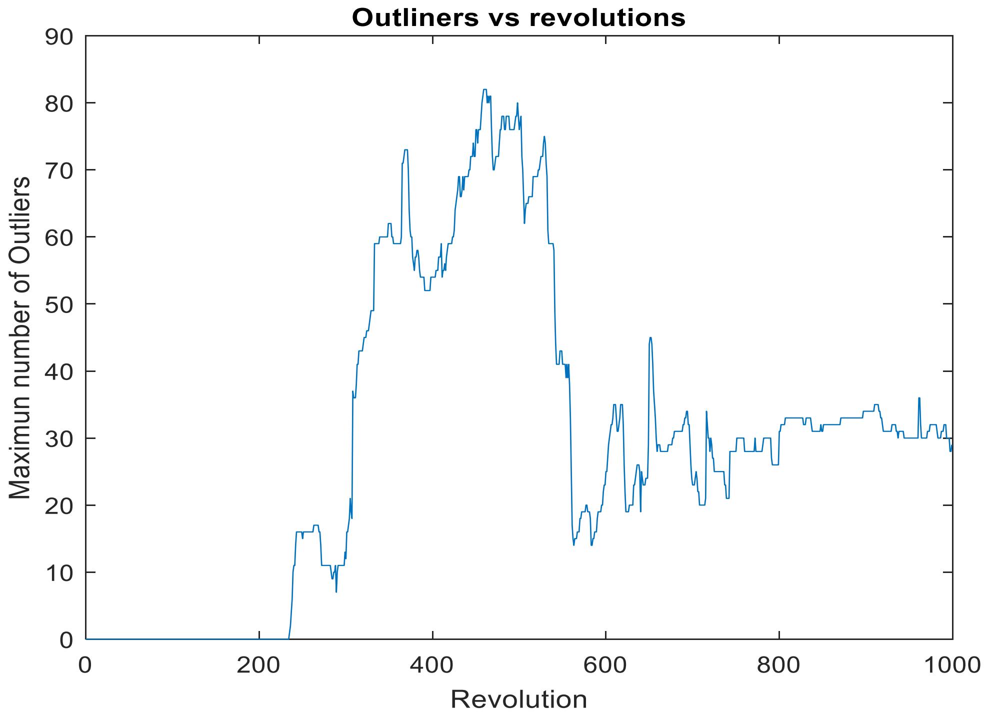

Figure 40 4^{th} eigenvalue of ESD model.

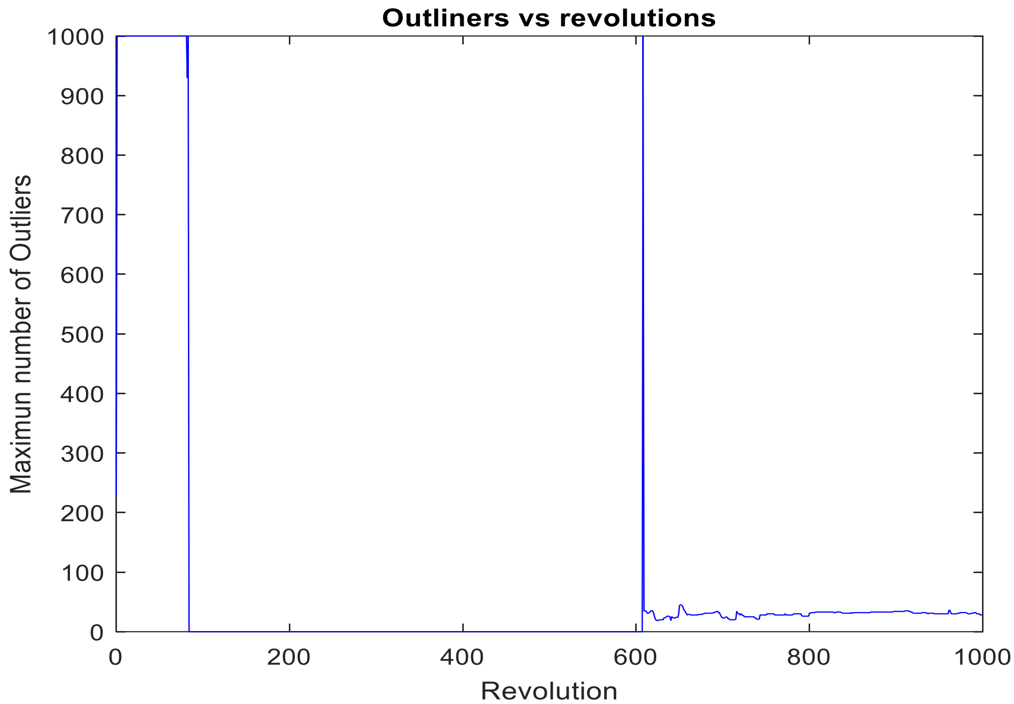

Figure 41 5th eigenvalue of ESD model.

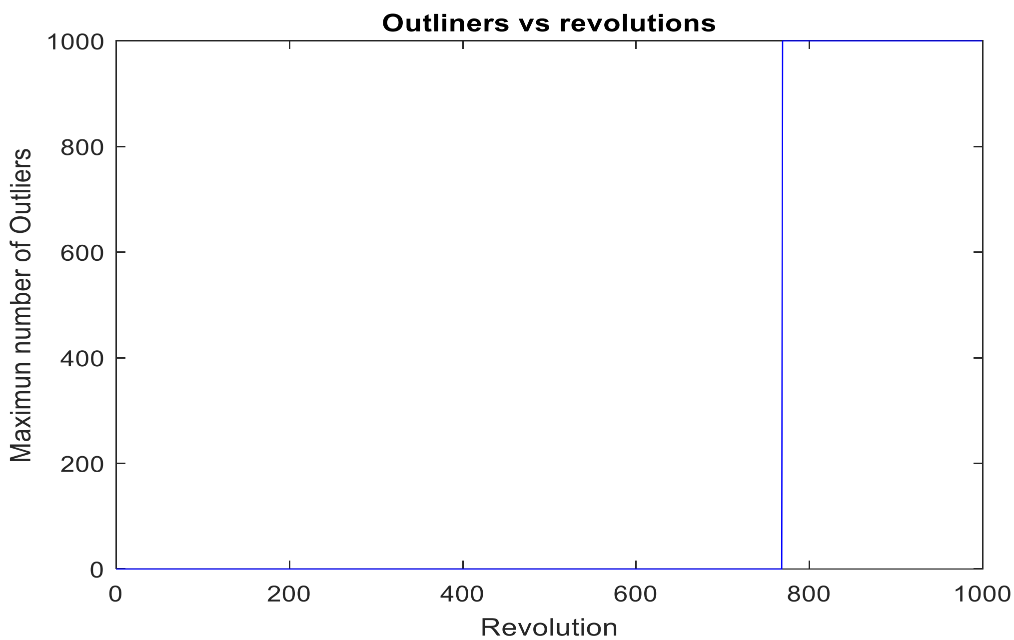

Figure 42 6th eigenvalue of ESD model.

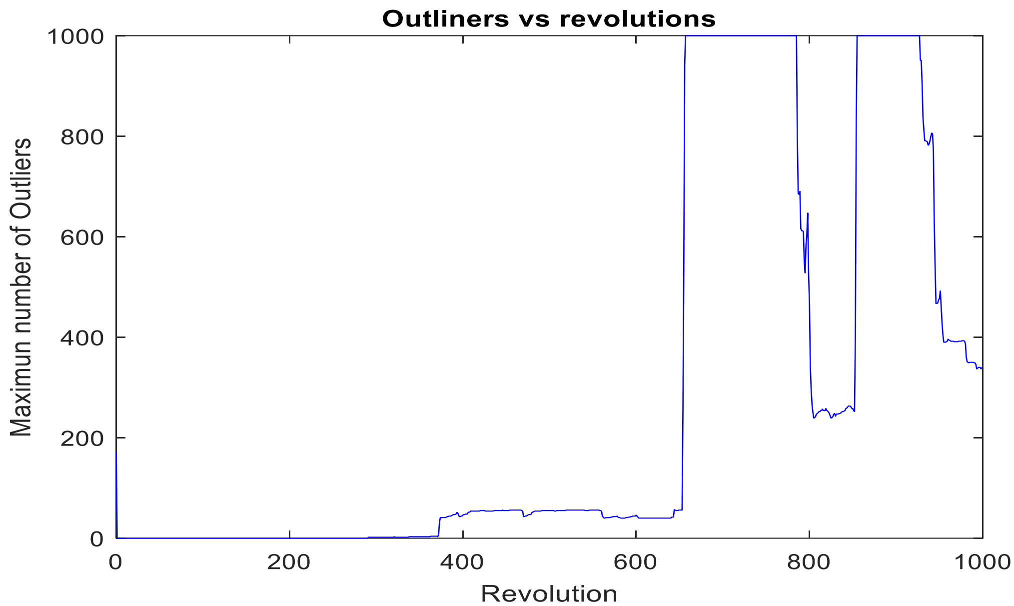

Figure 43 7th eigenvalue of ESD model.

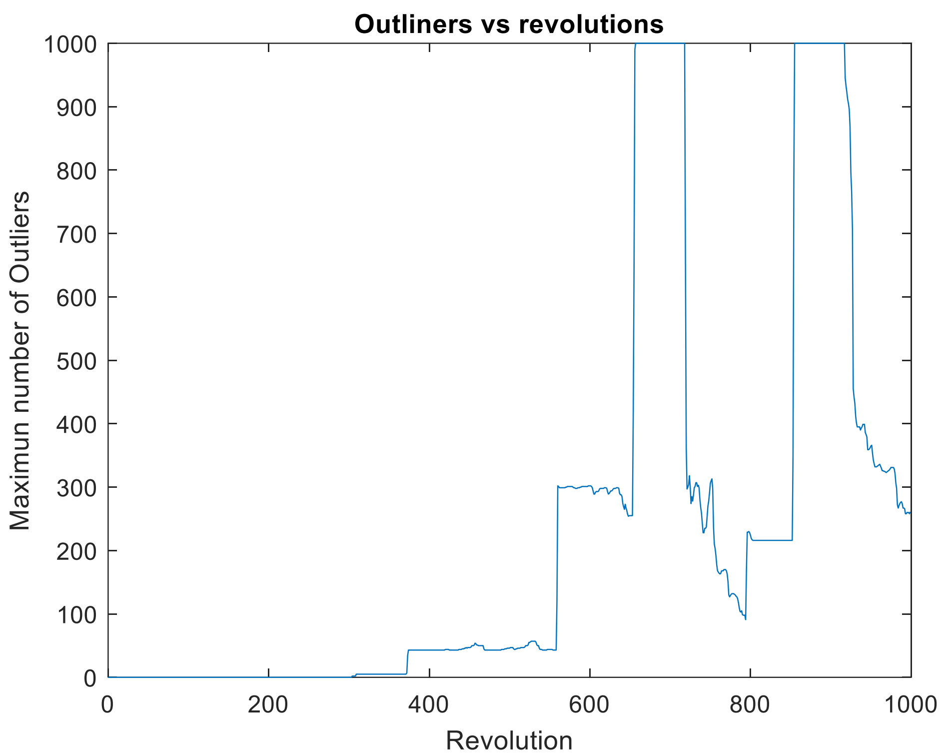

Figure 44 8th eigenvalue of ESD model.

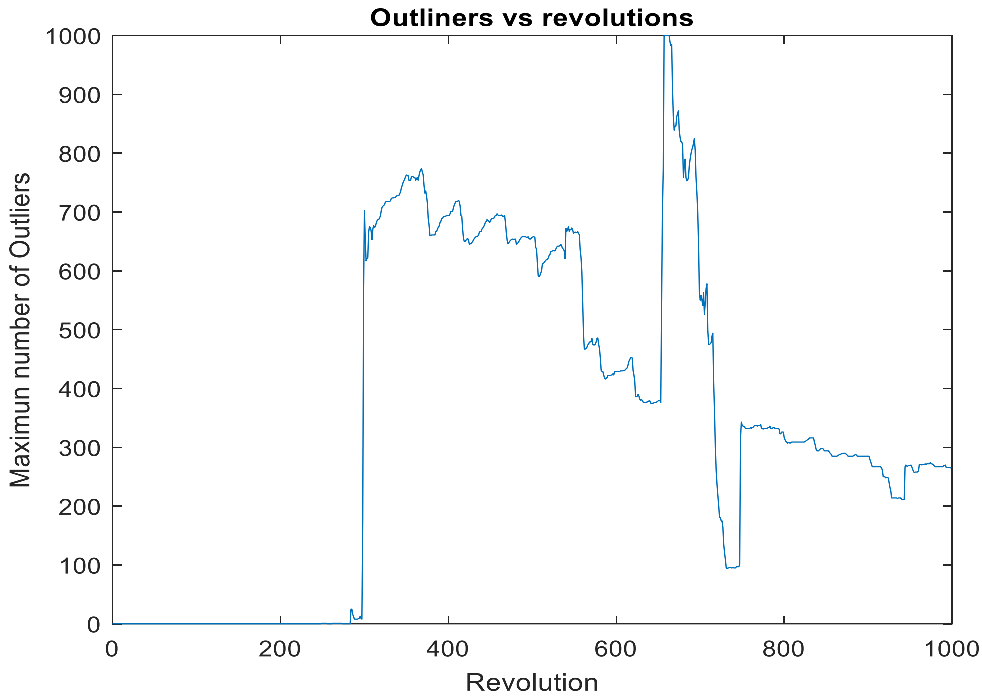

Figure 45 9th eigenvalue of ESD model.

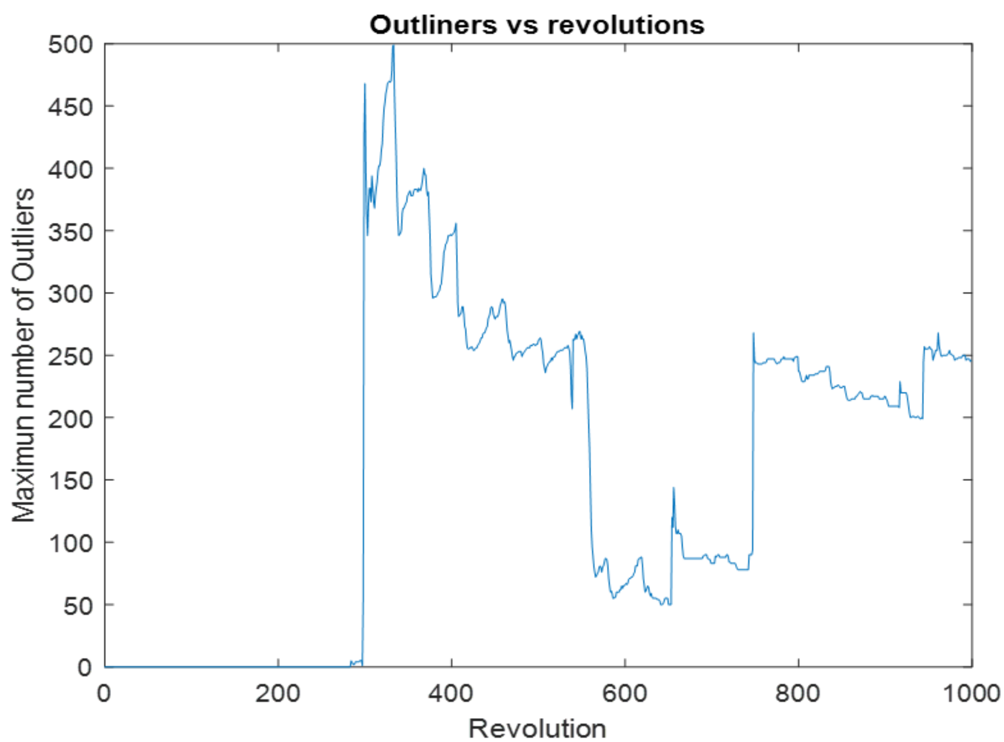

Figure 46 10th eigenvalue of ESD model.

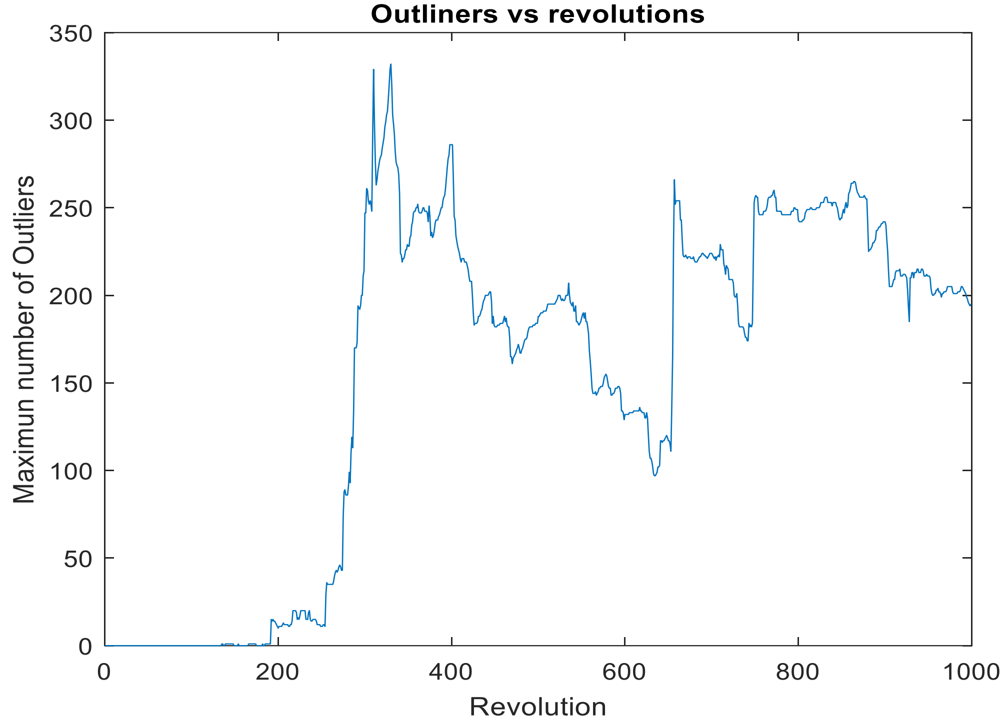

Figure 47 11th eigenvalue of ESD model.

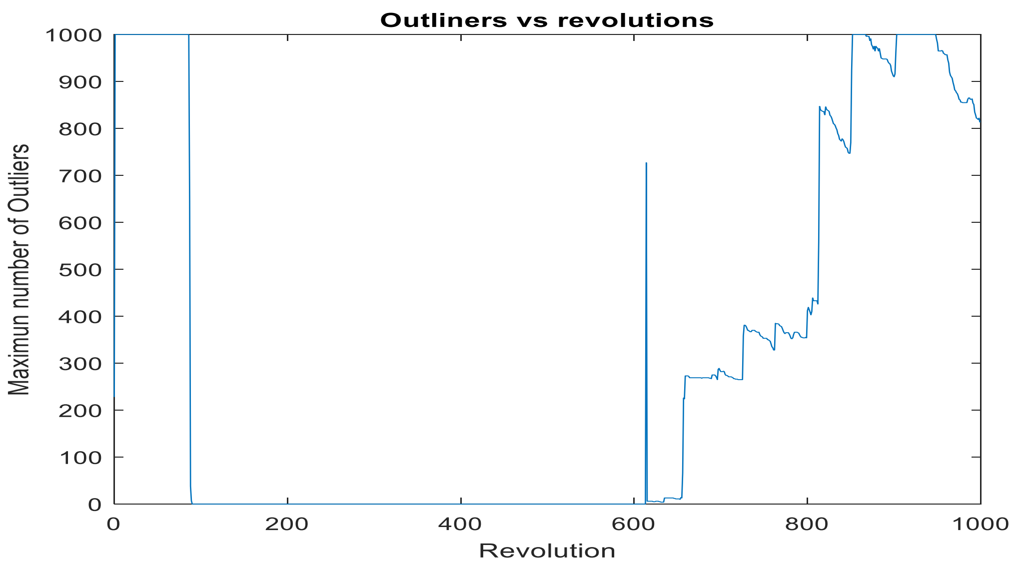

Figure 48 12th eigenvalue of ESD model.

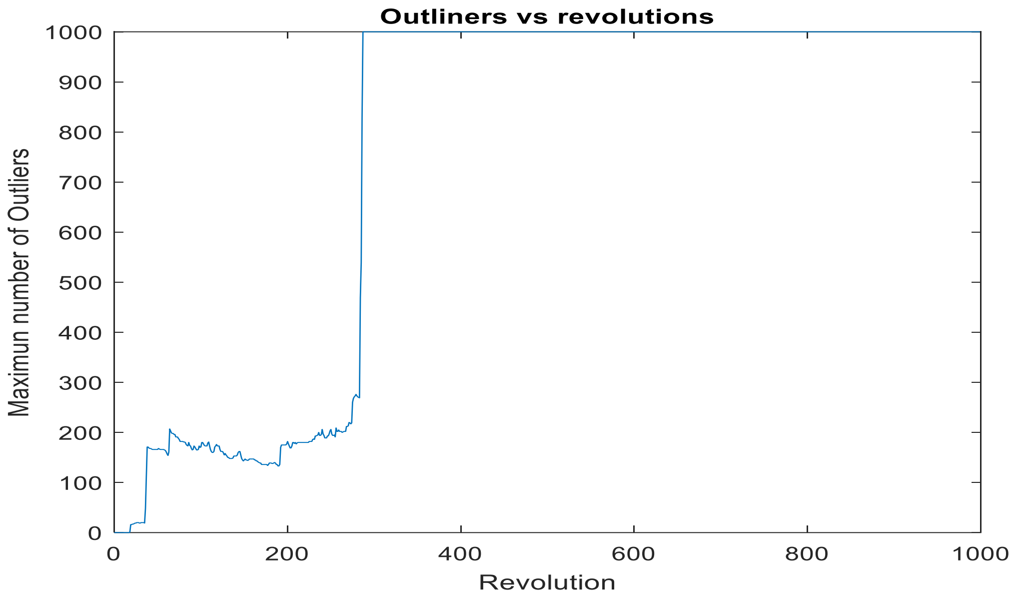

Figure 49 13th eigenvalue of ESD model.

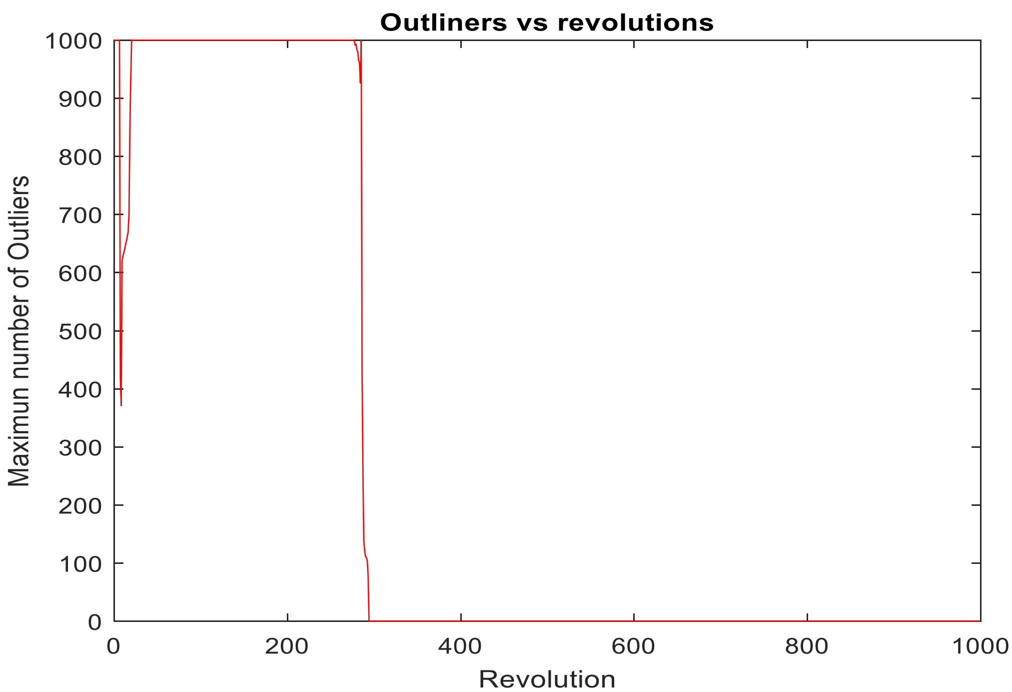

Figure 50 14th eigenvalue of ESD model.

5.5 Conclusions

This paper presents a numerical study for spike stall and surge issues in the jet engine's compressor. An Autoregression model (AR) and an ESD test were developed to test pressure data collected from the running compressor in different operation conditions. The Autoregression model indicates the pressure data that close to have a spike stall in the compressor's operation. The Autoregression model defines the eigenvalues matrix of the pressure data collected from the leading tip edge of the compressor's blades. Each eigenvalue tested using an ESD test to indicate which eigenvalue the spike stall was close to in the compressor operation. The (AR) model can predict the spike stall and surge close to happen in the jet engine operation. Also, the ESD test is capable of indicating which eigenvalue is close to having a stall happening. It has been shown that the ESD test and (AR) model capabilities can predict the spike stall issue in the compressor, which will lead to the capability to increase the operating the jet engine efficiency.

5.6 Future Work

Future research will be facilitated by the J34 WE-36 jet engine system that was constructed by Idaho State University students. A pressure sensor will be attached to the J34 WE-36 compressor, while the main shaft of the compressor is driven by an electric motor in order to run the J34 WE-36 for experimental pressure data collection. After the data is collected from the 34 WE-36 compressor, an Autoregression model will be extracted and the ESD routine applied for the purpose of detecting precursors identified by the behavior of the AR model's eigenvalues. In addition, different mathematical models can be utilized and investigated to capture the characteristics of the dynamics of the compressor and hence the onset of stall for its detection. These measures are necessary tasks to ultimately implement active flow control for mitigating the onset of stall and hence increasing the efficiency of the jet engine operation.

Reference

1. Seas, T. (2016). Stall of the wing. Retrieved November 02, 2020, from this link.
2. A Study of Spike and Modal Stall Phenomena in a Low-speed Axial Compressor. (1998). Web link
3. Paduano,J., Greitzer, E., & Epstein, A. (2001). Compression System Stability and Active Control. Annual Review of Fluid Mechanics, 33, 491.
4. Pratt and Whitney Aircraft. (1957). Handbook Overhaul Instructions: Navy Model J34-We-36A Aircraft Engine Direction of the Commander of the Naval Air Systems Command.
5. Carol Hodanbosi, C. (1996). 3RD LAW OF MOTION. Retrieved October 31, 2020, from this link.
6. Vo, H. D. (2001). Role of tip clearance flow on axial compressor stability. Massachusetts, *MA: Massachusetts Institute Of Technology.
7. Xiaochen Mao, Bo Liu, & Hang Zhao. (2017), Numerical Investigation for the Impact of Single Groove on the Stall Margin Improvement and Unsteadiness of Tip Leakage Flow in a Counter-Rotating Axial Flow Compressor. Energies (19961073), 10(8), 1153
8. Anderson, J. D. (2017). Fundamentals of Aerodynamics. New York, NY: McGraw Hill Education.
9. Montgomery, S. R. (2012). An Investigation of Rotating Stall in a Single Stage Axial Compressor.

10. Zhiqiang, W., Jiaxin, L., & Luo, C. (2018). Numerical Study on the Stall Process if a Low Speed Axial Compressor Rotor. 2018 15th International Bhurban Conference on Applied Sciences and Technology (IBCAST).

11. Huu Duc Vo. (2007). Active Suppression of Rotating Stall Inception with Distributed Jet Actuation. International Journal of Rotating Machinery, 2007. Web link

12. Wirkowski. (2007). Modelling the Characteristics of Axail Compressor of Variable Flow Passage Geometry, Working in the Gas Turbine Engine System. Polish Maritime Research, 14(3), 27-32.

13. Pullan, G., Young, A. M., Day, I. J., Greitzer, E. M., & Spakoyszky, Z. S. (2015). Origins and Structure of Spike-Type Rotating Stall. Journal of Turbomachinery, 137(5).

14. Zhao JiaYim Xi Guang. Wang ZhiHeng, & Zhao Yang. (2018). The Role of Tip Leakage Science China Technological Sciences, 61(6), 830-842. Web link

15. J. PADUANO, A. H. EPSTEIN, L. VALAVANI, J. P. LONGLEY *, E. M. GREITZER, & G. R. GUENETTE. (1991). Active Control of Rotating Stall in a Low Speed Axial Compressor. Gas Turbine Laboratory Massachusetts Institute of Technology.

16. The Role of Tip Leakage Flow in Spike-Type Rotating Stall Inception. (2018).

17. Eighdi Aung, Marco P. Schoen, & Jichao Li. (2019). Application of Statistical Measures for the Precursor Detection of Spike Stall in Axial Compressor System: Idaho State University.

18. Zhiqiang, W., Jiaxin, L., & Luo, C. (2018). Numerical Study on the Stall Process if a Low Speed Axial Compressor Rotor. 2018 15th International Bhurban Conference on Applied Sciences and Technology (IBCAST). 673-681.

19. V. H. Garnier, A. H. Epstein, & E. M. Greitzer (1991). Rotating Waves as a Stall Inception Indicatoin in Axial Compressor. Gas Turbine Laboratory Massachusetts Institute of Technology

20. Hoying, D., Tan, C., Vo, H., & Greitzer, E. (n.d.). Role of Blade Passage Flow Structures in Axial Compressor Rotating Stall Inception. Journal of Turbomachinery Transactions of the ASME, 121(4), 735-742.

21. Frank E. Grubbs. (1950). Sample Criteria for Testing Outlying Observation. The Annals of Mathematical Statistics, 21(1), 27.

22. Is it possible for jet engines to have no moving parts? - Quora. (2020). Will Simmons. https://www.quora.com/Is-it-possible-for-jet-engines-to-have-no-moving-part

23. Wirkowski, P. (2007). Modeling the Characteristics of Axial Compressor of Variable Flow Passage Geometry, Working in the Gas Turbine Engine System Polish Maritime Research, 14(3), 27-32. Web link.

24. Sears, W.R. Rotating stall in axial compressors. Journal of Applied Mathematics and Physics (ZAMP) **6,** 429–455 (1955). https://doi.org/10.1007/BF01600530

Appendix

Autoregressive model to create the eigenvalue and plot them

```
%% Auto Regression
A1=A0505stall(:,2);  % using file data A_052
% sliding window-alogrithm
% first we need to know the width of the window
width=2461; % with of the window we get for  m m the code
AliTest2 is the number of window
[ndp,ncol]=size(A1);
noi=ndp-width; %
for s=1:1:noi % S is the victor position
    v=1;      %
    for t=s:1:s+width-1
    D(v,s)=A1(t,1);
    v=v+1;
    end
end
[a,b]=size(D);
T=zeros(14,10); %  is the number of eignvalue
for k=1:1:b % k is the number of windows
    k
B=(D(:,k))';
p=15;
Y=B;[no,L]=size(Y);
V=zeros((L-p),p); % Define matrix theta as V
Yar=Y(:,p+1:L)';%initialize variables for speed
for j=p+1:L
   for c=1:p
      V(j-p,c)=Y(:,j-c);
   end
end
Z=V'*V;
Theta=inv(Z)*V'*Yar;
Theta1=abs(roots(Theta));
T(:,k)=Theta1;
Ts=T';
R=Yar-V*(Theta); % developed loop to calculate the peak
end

[Ro,Co]=size(Ts);
for i=1:Ro
    x(i)=i;
end
figure (1) % plot the eigenvalue vs the revolution most
important plot
```

```
hold on
plot(x,Ts(:,1),'b')
title('Eigenvalue vs Revolutions')
xlabel('Revolutions ')
ylabel('Correlation Coefficient')
hold off
```

ESD test model to indicate the spike stall eigenvalue:

```
%% Autocorrelation ESD test
A1=Ts(:,6) % Ts is produced from Ar_threestage file
[g h]=size(A1);
avgndp=457; % averaged is from the reserch paper is 457
%growing window method
gr=avgndp;%the rate at which we want to increase the size of the
window gr=n points per iteration
off=avgndp;
noi=(floor(g/avgndp)-1)*avgndp; %number of revolutions to check
esd=1;
for a=off:gr:noi  % noi is the number of the revolution per
window
    c=1;
    for b=1:1:a
        if b<g
        B(c,1)=A1(b,1);
        c=c+1;
        end
    end
        %% ESD in general
        alpha=0.05;
        [n m]=size(B);
        if n<=avgndp
            o=avgndp/2;
        end
        if n>avgndp*3
            o=1000;
        end
        for d=1:1:o  %Check all the window
            [n m]=size(B);
            l=d-1;
            nu=n-l-2;
                                    %First fourmal to compare
            p=1-(alpha/(2*(n-l)));  %We will calculate the
percentil of the t-distribution
            t= tinv(p,nu);          %
            lambda=(t*(n-l-1))/(((nu+(t^2))*(n-l))^(0.5));
            lambdamat(d,1)=lambda; %Critical values
            avg=mean(B);
            sigma=std(B);
```

```
            e=1;
            for e=1:1:n
                C(e,1)=abs((B(e,1)-avg)/sigma); %Maximun
outliers presented in this window (R)
            end
            Cmax=max(C);   %Select max
            X=find(C(:,1)==Cmax); %Get the linear indix where is
the maximum
            C=zeros(n-1,1); % For the new one
            outlier=B(X(1,1),1); %Get the value of B that
correspond  with the maximum
            outliermat(d,1)=Cmax; %vector of outliers
            B=B(find(B~=outlier(1,1)));
            compare(d,1)=d;
            compare(d,2)=outliermat(d,1); % second compartion
            compare(d,3)=lambdamat(d,1);
        end
        %check the compare matrix for max number of outliers
        %Get the value of the max outlier of the window
        [c1 c2]=size(compare);
        e1=1;
        E=zeros(c1,3);
        for u=1:1:c1 %Until the number of rows
            if compare(u,2)>compare(u,3)  %What is bigger? the
value from lambda or from max{i:Ri>lambdai}
                E(e1,:)=compare(u,:);
                e1=e1+1;
            else
                E(e1,1)=0;
                E(e1,2)=0; % Devloping matrix for building the
algorthim
                E(e1,3)=0;
                e1=e1+1;
            end
        end
        ESD(esd,1)=max(E(:,1)); %The outier
        esd=esd+1;
end

%% Plot the results
[row, col]=size (ESD)   % Get the number of rows ans columns
X_axis=[0:1:row-1]';
figure (3)
plot(X_axis, ESD,'b')
title('Outliners vs revolutions')
xlabel('Revolution')
ylabel('Maximun number of Outliers')
```

Plot the Pressure Data to Compare Between the Pressure Plot and the Eigenvalue Plot

```
figure (1)
plot(A,'r')
title('Pressure vs Revolutions')
xlabel('Revolutions ')
ylabel('Pressure')
figure (3)
plot(X_axis, ESD)
title('Outliners vs revolutions')
xlabel('Revolution')
ylabel('Outliers')
figure (2) % plot the eigenvalue vs the revolution most
important plot

plot(x,Ts(:,14),'m')
title('Eigenvalue vs Revolutions')
xlabel('Revolutions ')
ylabel('Eigenvalue 14')

figure(4)
plot (Theta1)
title('Theta1')
```

Filter the Pressure Data and Filter the Revolution

```
avgndp=457;
B=A0505stall(:,1);
[a b]=size(B);
map1=floor(a/avgndp);
for i=1:1:a
    Mapped1(i,1)=map1*(i/a);
    Mapped1(i,2)=B(i,1);
end
x=Mapped1(:,1);
y=Mapped1(:,2);
plot(x,y,'k')
ylim([min(B) max(B)])
xlabel('Revolutions')
ylabel('Pressure [units of pressure]')
title('Pressure vs Revolutions')
```

ESD Model

```
%% Autocorrelation ESD test
A1=Ts(:,6) % Ts is produced from Ar_threestage file
[g h]=size(A1);
avgndp=457; % averaged is from the reserch paper is 457
%growing window method
```

```
gr=avgndp;%the rate at which we want to increase the size of the
window gr=n points per iteration
off=avgndp;
noi=(floor(g/avgndp)-1)*avgndp; %number of revolutions to check
esd=1;
for a=off:gr:noi  % noi is the number of the revolution per
window
    c=1;
    for b=1:1:a
        if b<g
        B(c,1)=A1(b,1);
        c=c+1;
        end
    end
        %% ESD in general
        alpha=0.05;
        [n m]=size(B);
        if n<=avgndp
            o=avgndp/2;
        end
        if n>avgndp*3
            o=1000;
        end
        for d=1:1:o  %Check all the window
            [n m]=size(B);
            l=d-1;
            nu=n-l-2;
                                    %First fourmal to compare
            p=1-(alpha/(2*(n-l)));  %We will calculate the
percentil of the t-distribution
            t= tinv(p,nu);          %
            lambda=(t*(n-l-1))/(((nu+(t^2))*(n-l))^(0.5));
            lambdamat(d,1)=lambda; %Critical values
            avg=mean(B);
            sigma=std(B);
            e=1;
            for e=1:1:n
                C(e,1)=abs((B(e,1)-avg)/sigma); %Maximun
outliers presented in this window (R)
            end
            Cmax=max(C);   %Select max
            X=find(C(:,1)==Cmax); %Get the linear indix where is
the maximum
            C=zeros(n-1,1); % For the new one
            outlier=B(X(1,1),1); %Get the value of B that
correspond  with the maximum
            outliermat(d,1)=Cmax; %vector of outliers
```

```
            B=B(find(B~=outlier(1,1)));
            compare(d,1)=d;
            compare(d,2)=outliermat(d,1); % second compartion
            compare(d,3)=lambdamat(d,1);
        end
        %check the compare matrix for max number of outliers
        %Get the value of the max outlier of the window
        [c1 c2]=size(compare);
        e1=1;
        E=zeros(c1,3);
        for u=1:1:c1 %Until the number of rows
            if compare(u,2)>compare(u,3)  %What is bigger? the
value from lambda or from max{i:Ri>lambdai}
                E(e1,:)=compare(u,:);
                e1=e1+1;
            else
                E(e1,1)=0;
                E(e1,2)=0; % Devloping matrix for building the
algorthim
                E(e1,3)=0;
                e1=e1+1;
            end
        end
        ESD(esd,1)=max(E(:,1)); %The outier
        esd=esd+1;
end

%% Plot the results
[row, col]=size (ESD)   % Get the number of rows ans columns
X_axis=[0:1:row-1]';
figure (3)
plot(X_axis, ESD,'b')
title('Outliners vs revolutions')
xlabel('Revolution')
ylabel('Maximun number of Outliers')
```

Autocorrelation

```
A=Ts(:,1);
[a b]=size(A);
w=2285;
ncol=floor(a/w);
for i=1:1:ncol
    b=1;
    for j=((i-1)*w)+1:1:i*w
    B(b,i)=A(j,1);
    b=b+1;
```

```
    end
end
y=1;
for x=1:1:i
    if x~=i
    compare1=[];
    compare2=[];
    compare1=B(:,x);
    compare2=B(:,x+1);
    Corrcoefficient2=corrcoef(compare1,compare2);
    Cc(y,1)=Corrcoefficient2(2,1);
    y=y+1;
    end
 end
A=Ts(:,1);
[a b]=size(A);
w=457;
ncol=floor(a/w);
for i=1:1:ncol
    b=1;
    for j=((i-1)*w)+1:1:i*w
    B(b,i)=A(j,1);
    b=b+1;
    end
end
y=1;
for x=1:1:i
    if x~=i
    compare1=[];
    compare2=[];
    compare1=B(:,x);
    compare2=B(:,x+1);
    Corrcoefficient2=corrcoef(compare1,compare2);
    Cc(y,1)=Cor62rcoefficient2(2,1);
    y=y+1;
    end
 end
```

Eigenvalue of AR System of Non-stall Data

First

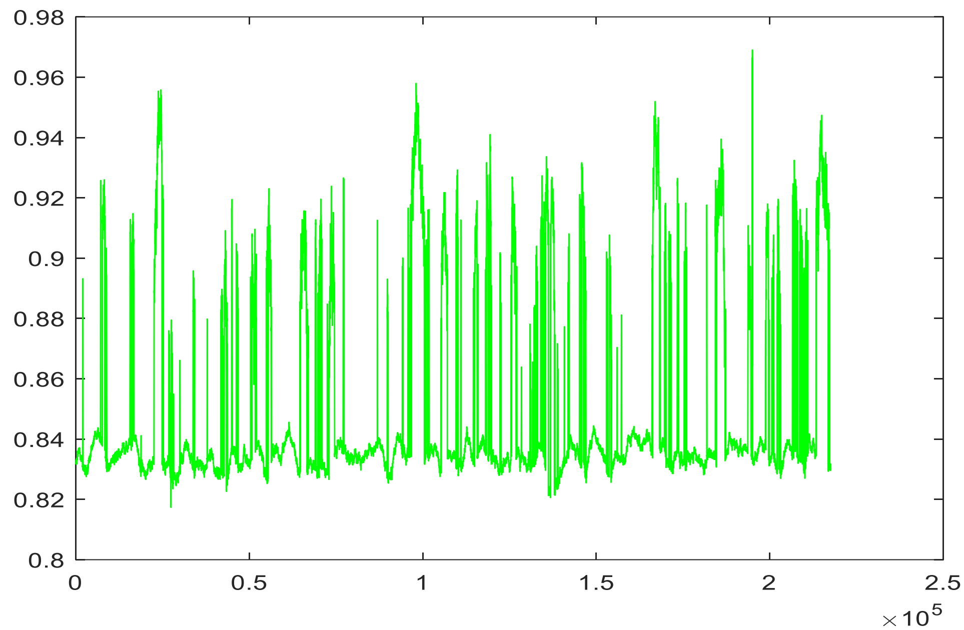

Second

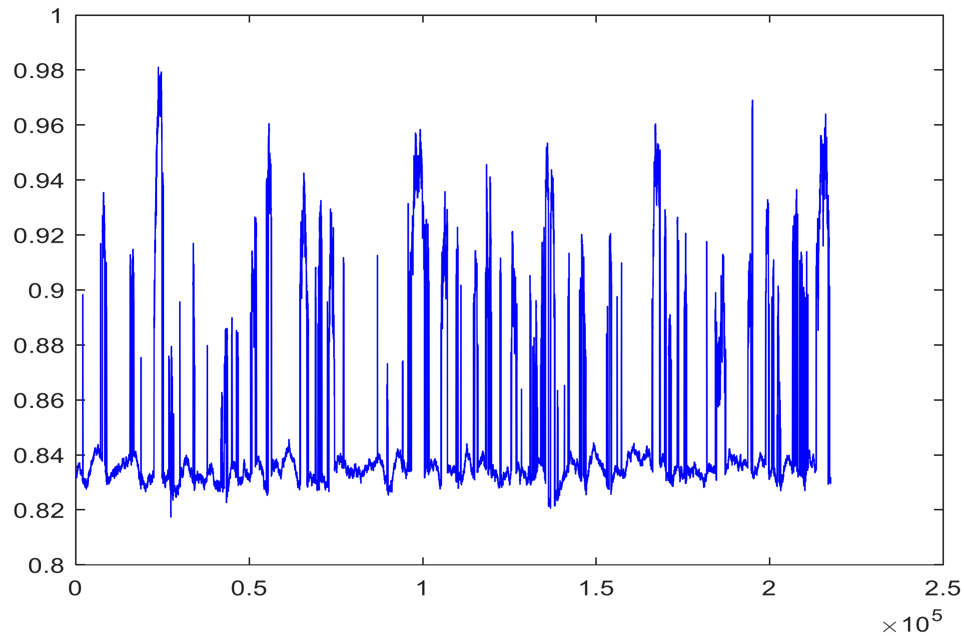

Third

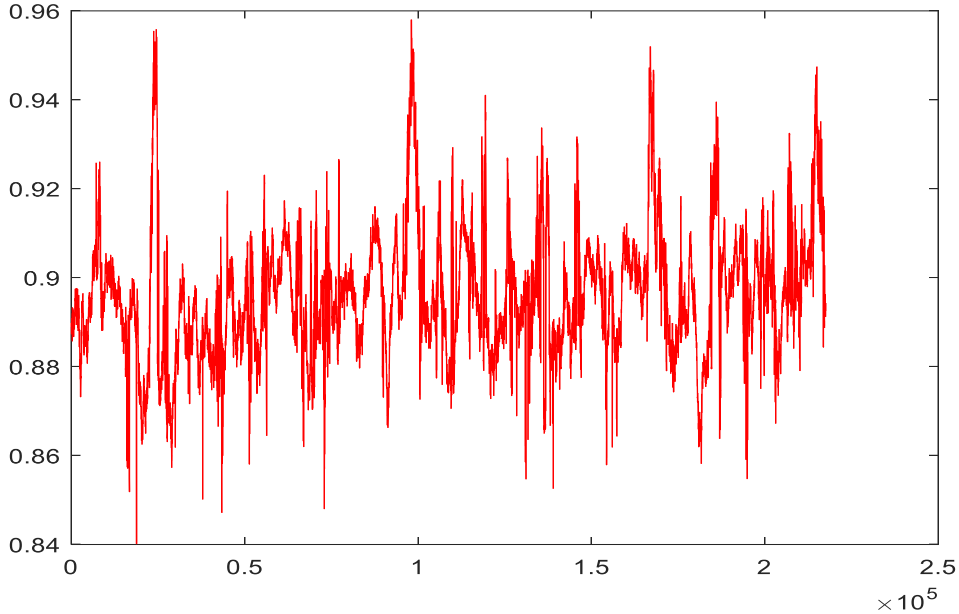

Fourth

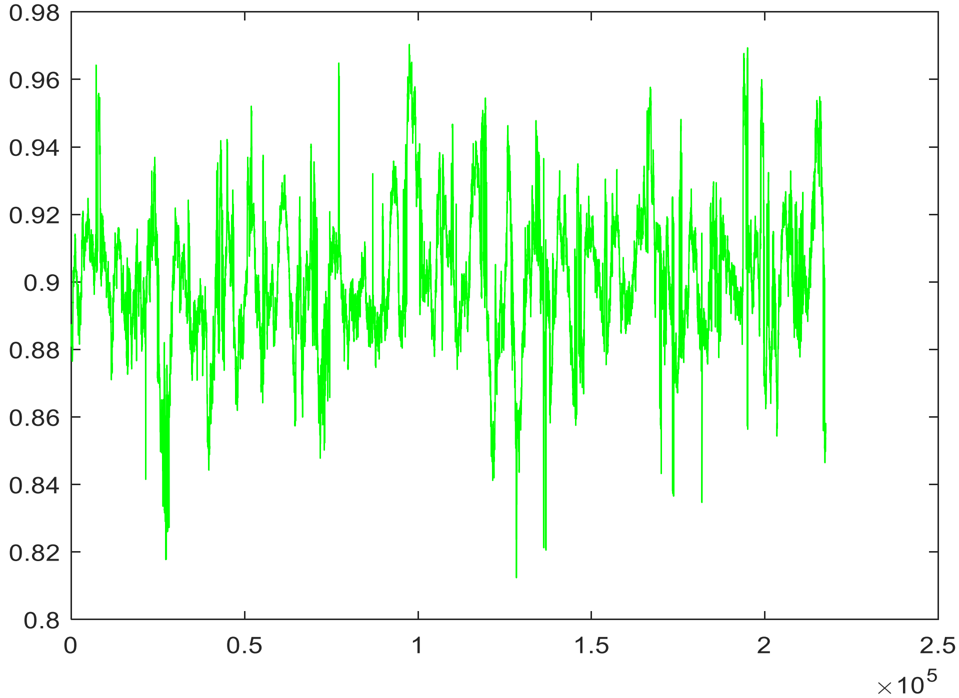

5th

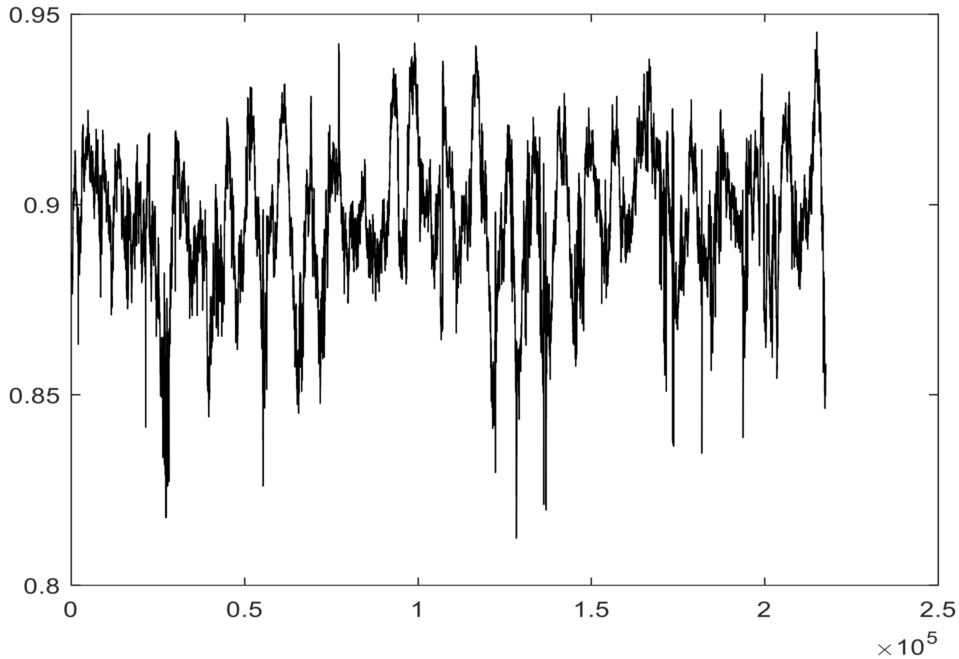
0.95
0.9
0.85
0.8
0
0.5
1
1.5
2
2.5
$\times 10^5$

6th

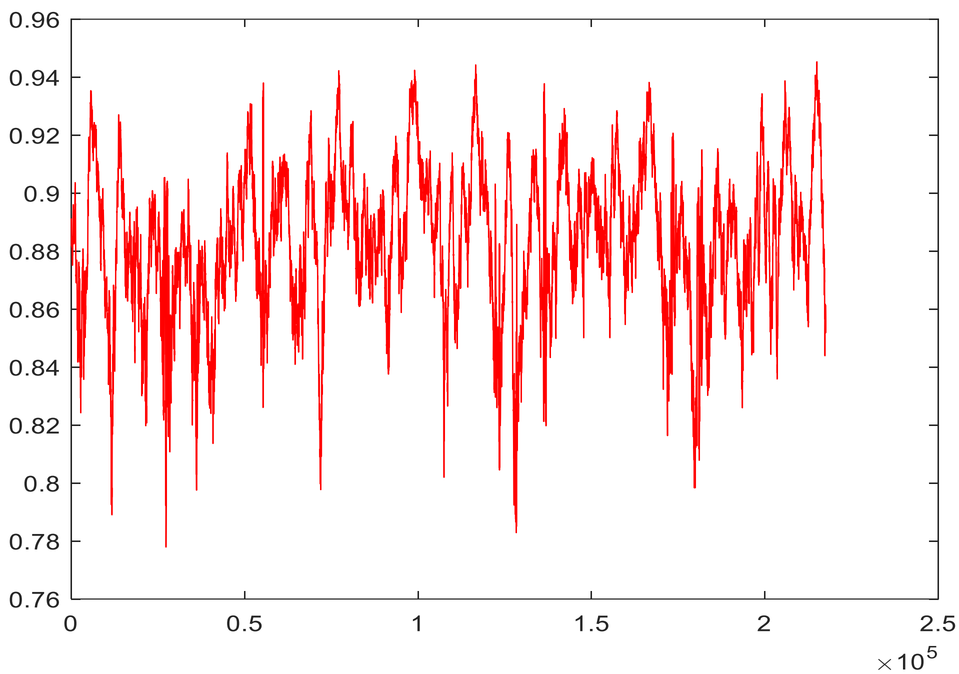
0.96
0.94
0.92
0.9
0.88
0.86
0.84
0.82
0.8
0.78
0.76
0
0.5
1
1.5
2
2.5
$\times 10^5$

7th

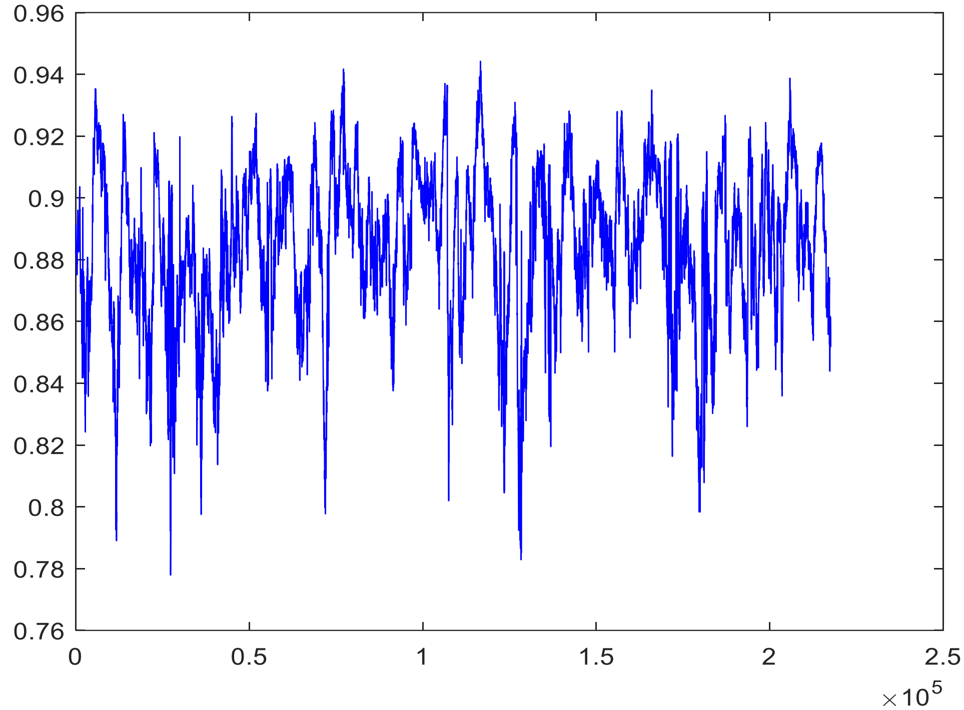
0.96
0.94
0.92
0.9
0.88
0.86
0.84
0.82
0.8
0.78
0.76
0
0.5
1
1.5
2
2.5
$\times 10^5$

8th

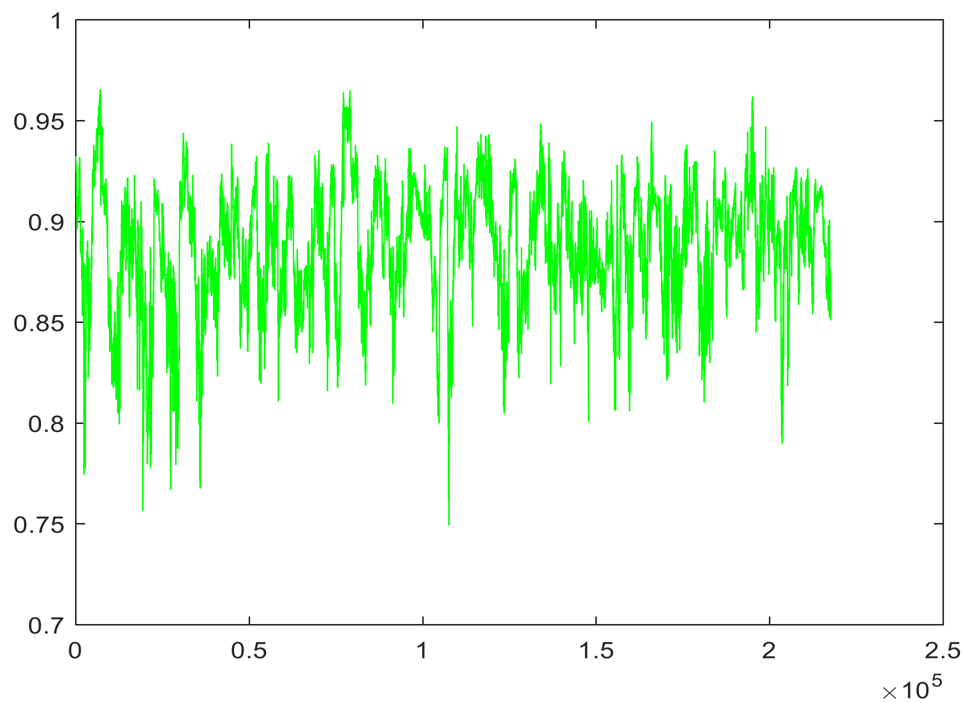
1
0.95
0.9
0.85
0.8
0.75
0.7
0
0.5
1
1.5
2
2.5
$\times 10^5$

9th

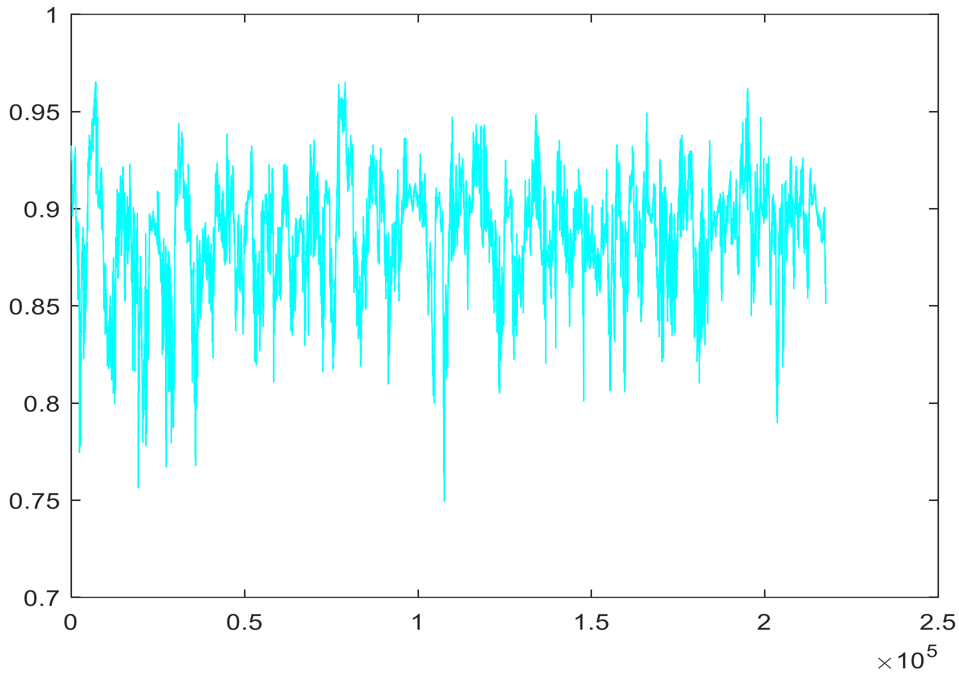

1
0.95
0.9
0.85
0.8
0.75
0.7
0
0.5
1
1.5
2
2.5
$\times 10^5$

10th

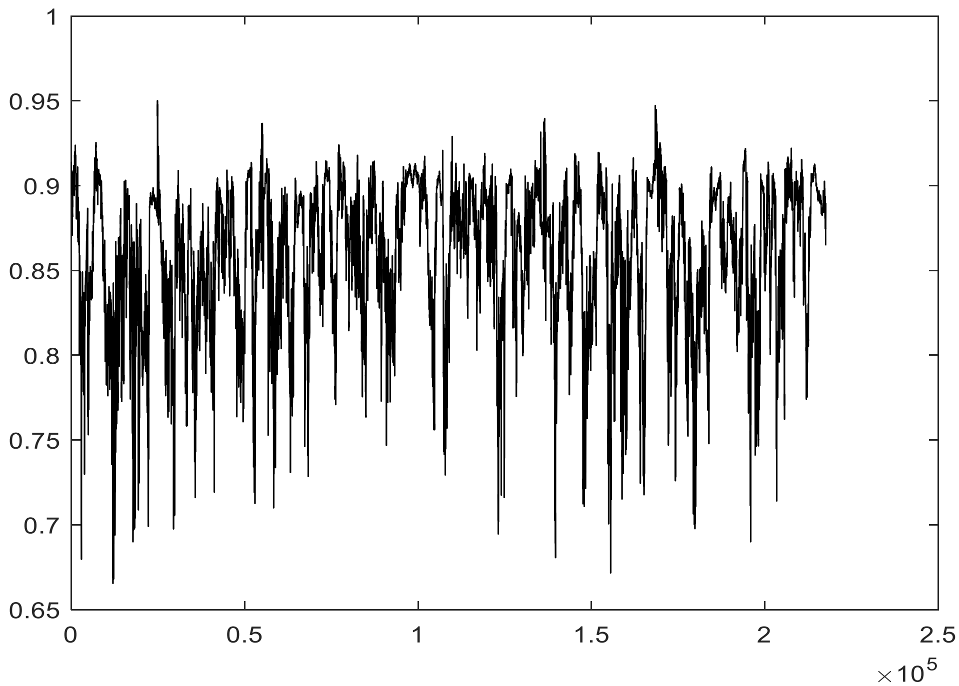

1
0.95
0.9
0.85
0.8
0.75
0.7
0.65
0
0.5
1
1.5
2
2.5
$\times 10^5$

11th

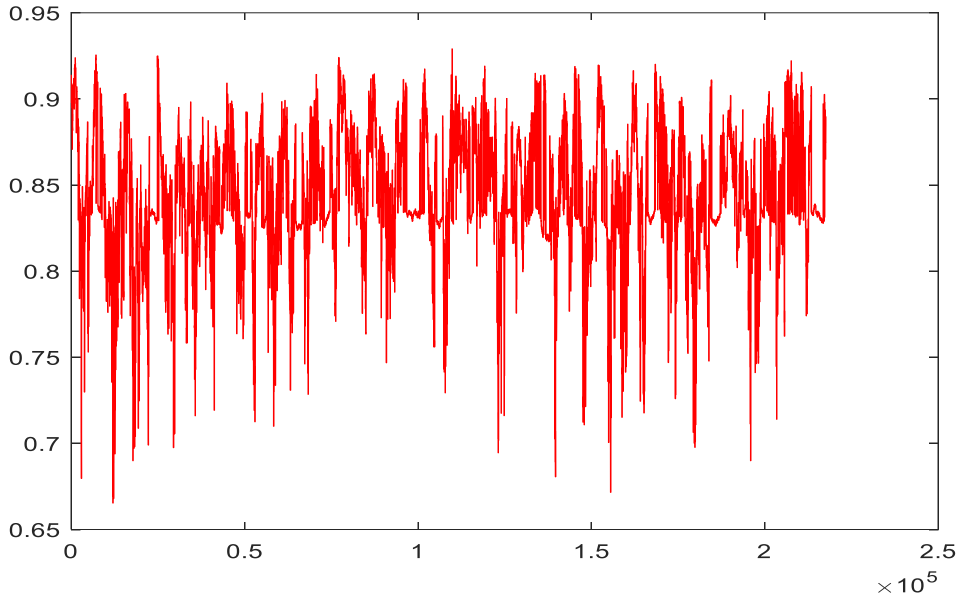
0.95
0.9
0.85
0.8
0.75
0.7
0.65
0
0.5
1
1.5
2
2.5
×10^5

12th

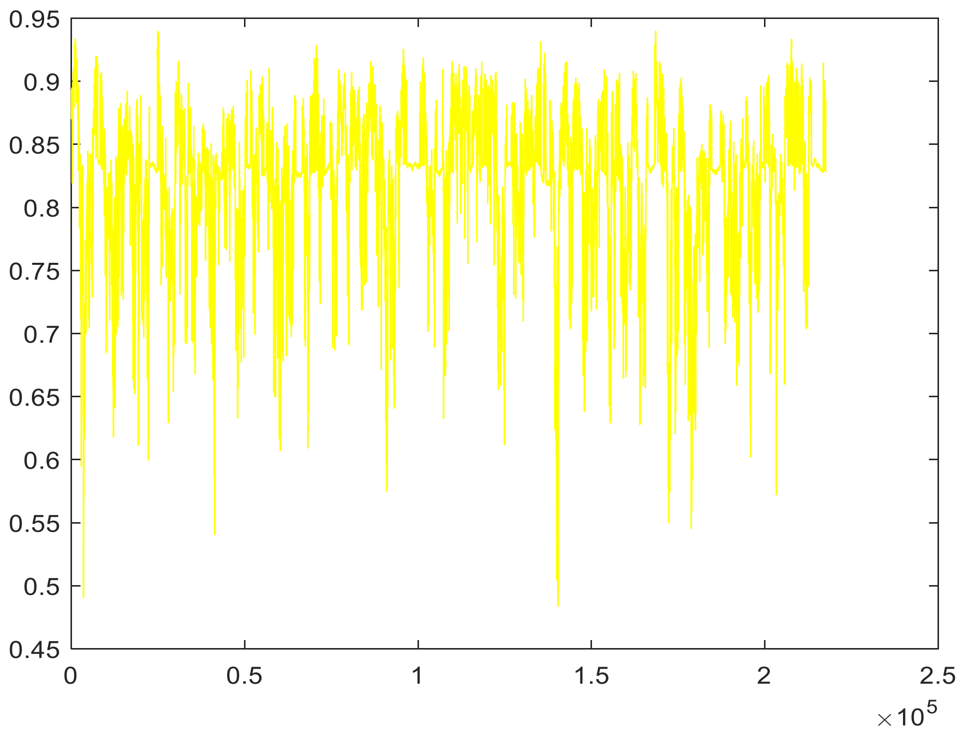
0.95
0.9
0.85
0.8
0.75
0.7
0.65
0.6
0.55
0.5
0.45
0
0.5
1
1.5
2
2.5
×10^5

14th